Analyzing Acute Psychosocial Stress Responses: A Video-Based Motion Analysis Approach

Bachelor's Thesis in Computer Science

submitted
by

Leon Schmid

born 05.05.1999 in Ansbach

Written at

Machine Learning and Data Analytics Lab
Department Artificial Intelligence in Biomedical Engineering
Friedrich-Alexander-Universität Erlangen-Nürnberg (FAU)

in Cooperation with

Chair of Health Psychology
Friedrich-Alexander-Universität Erlangen-Nürnberg (FAU)

Ich versichere, dass ich die Arbeit ohne fremde Hilfe und ohne Benutzung anderer als der angegebenen Quellen angefertigt habe und dass die Arbeit in gleicher oder ähnlicher Form noch keiner anderen Prüfungsbehörde vorgelegen hat und von dieser als Teil einer Prüfungsleistung angenommen wurde. Alle Ausführungen, die wörtlich oder sinngemäß übernommen wurden, sind als solche gekennzeichnet.
Die Richtlinien des Lehrstuhls für Bachelor- und Masterarbeiten habe ich gelesen und anerkannt, insbesondere die Regelung des Nutzungsrechts.

Erlangen, den 20. März 2024

Übersicht

Stress kann zu einer Vielzahl von, zum Teil schwerwiegenden, gesundheitlichen Folgen führen. Um Stressreaktionen zu messen, werden bestimmte Biomarker wie Cortisol, Alpha-Amylase (α-Amylase) und Entzündungswerte im Labor anhand von Blut- oder Speichelproben bestimmt. Diese Methoden liefern zuverlässige Ergebnisse, sind jedoch komplex und arbeitsintesiv, was sie teuer und begrenzt skalierbar machen. Es wäre daher von Vorteil, alternative Verfahren zu entwickeln, die diese Nachteile nicht haben. In der Stressforschung wäre es außerdem wünschenswert, dass diese Techniken berührungslos und nicht-invasiv sind, damit sie das natürliche Verhalten der Person so wenig wie möglich beeinflussen. Ein dabei vielversprechender Ansatz ist die Analyse von Körperhaltung und Bewegungen als akute psychosoziale Stressreaktion.

Um die Forschung zur berührungslosen Stresserkennung zu unterstützen, wurde eine Studie durchgeführt, bei der Körperbewegungen und -haltung während einer akuten Stresssituation mit einer Videokamera aufgezeichnet wurden. Insgesamt wurden einhundertundeins Teilnehmer an zwei aufeinanderfolgenden Tagen und in zufälliger Reihenfolge dem "Trier Social Stress Test" (TSST) und einer modifizierte Version des "friendly-Trier Social Stress Test" (f-TSST) als stress-freie Kontrollbedingung im stehen oder sitzen unterzogen. Während des "(friendly-)Trier Social Stress Test" ((f-)TSST) wurde der gesamte Körper mit einer Azure Kinect und später mit einem Smartphone gefilmt. Die Videoaufnahmen wurden anschließend mit dem *openTSST*-Framework, einer webbasierten Plattform für videobasierte Bewegungsanalyse, entwickelt vom Machine Learning and Data Analytics Lab (MaD Lab) (Erlangen, Bayern), verarbeitet. Alle 2D-Positionen, die für bestimmte Körperteile für ein einzelnes Bild des Videos ermittelt wurden, wurden verwendet um eine Vielzahl von Bewegungsmerkmalen abzuleiten und statistisch zu analysieren. Wie in anderen Arbeiten wurde ein defensives "Freezing"-Verhalten, einem signifikanten Bewegungsrückgang, als Reaktion während dem TSST festgestellt. Nachgewiesen konnte dies im Hals- und Kopfbereich. Dies wurde jedoch nur bei den Teilnehmern beobachtet, die den (f-)TSST im Stehen durchführten. Für die sitzende Variante wurden keine Charakteristika gefunden, die eine Unterscheidung der beiden Bedingungen ermöglichten.

Darüber hinaus wurden geschlechtsspezifische Unterschiede bei der stehenden Variante untersucht, die darauf hindeuteten, dass sich Frauen in beiden Bedingungen tendenziell mehr im Hüftbereich bewegten. Außerdem wurden die einzelnen Phasen des TSST getrennt untersucht, was ein höheres Stressniveau während der Mathephase ergab. Dies wurde durch eine Verringerung der Bewegung in fast allen beobachteten Körperteilen quantifiziert. Zum Schluss wurde ein Machine Learning (ML)-Modell trainiert, um zwischen dem TSST und dem f-TSST zu klassifizieren, welches eine Genauigkeit von $68.5\% \pm 9.7\%$ erreichte.

Abstract

Stress can lead to a variety of partly severe health consequences. To measure stress responses, biomarkers such as cortisol, alpha-amylase (α-amylase), and inflammation levels are evaluated in the laboratory using blood or saliva samples. These methods provide reliable results but require complex procedures that demand trained personnel and are labor-intensive, making them expensive and limited in scalability. It would be advantageous to develop alternative techniques that do not have these drawbacks. In stress research, it would be desirable for these techniques to be contactless and non-invasive having as little impact as possible on the person's natural behavior. A promising approach is the analysis of body posture and movements as an acute psychosocial stress response.

To support research towards contactless stress detection, a study was conducted in which body movements and posture during an acute stress situation were recorded with a video camera. A total of one hundred and one participants performed the Trier Social Stress Test (TSST) and a modified version of the friendly-Trier Social Stress Test (f-TSST) as a stress-free control condition on two consecutive days and in a randomized order. In addition, there was a random allocation to a group, which determined whether the two tests would be carried out standing or sitting. During the (friendly-)Trier Social Stress Test ((f-)TSST), the entire body of the participant was filmed using a Microsoft Azure Kinect and later a cell phone. The video recordings were processed using the *openTSST* framework, a web-based platform for video-based movement analysis developed by the Machine Learning and Data Analytics Lab (MaD Lab) (Erlangen, Bavaria). All the 2D positions obtained for specific body parts for an individual frame of the video, were then used to derive and statistically analyze a variety of movement features. The expectation from previous work that participants would react with defensive freezing behavior during the TSST was quantified in this study by a significant decrease in movement throughout the neck and head area. However, this was only observable for the participants performing the (f-)TSST standing. For the seated variation, no characteristics that allowed the two conditions to be distinguished, were found.

Additionally, gender differences were investigated for the standing variation, which suggested that females tended to move more in the hip region in both conditions. Furthermore, the individual phases of the TSST were examined separately, which showed a higher stress level during the math phase. This was quantified by a decrease in movement in almost all observed body parts. Finally, a machine learning (ML)-model was trained to classify between the TSST and the f-TSST, which achieved an accuracy of $68.5\% \pm 9.7\%$.

Contents

Chapter 1

Introduction

Stress is an integral part of our daily lives, and although it is a necessary and healthy reaction of the body, excessive stress may have serious negative effects on our physical and mental well-being. This can be caused by direct effects, such as autonomic and neuroendocrine responses, or indirectly through changes to health behavior, e.g. introducing or maintaining harmful eating habits [OCo21]. Risks associated with stress include life-threatening physiological consequences such as insulin insensitivity, cardiovascular diseases, or cancer [Coh07], and different mental illnesses like depression or anxiety [Hal21]. Various consequences of stress as a mediating problem have already been identified, such as increased smoking, sleep, or eating disorders [Sch05]. Continuing with the example of smoking, a study by Conway et al. [Con81] showed that stress may additionally play a moderating role and, on average, more cigarettes were consumed on days with a higher stress level which in turn poses serious health risks like higher mortality of lung cancer and chronic obstructive pulmonary disorder [Col94]. Consequently, stress has been recognized as a significant cause of numerous long-term physical and mental illnesses in many countries [Hap13; APA20], and is a subject of extensive research [McE93].

To study stress responses, it is necessary to reliably trigger stress in participants. At present, the gold standard for inducing acute psychosocial stress in a laboratory setting is the TSST [Kir93] involving public speaking and a challenging arithmetic task. The f-TSST [Wie13] is used as a control condition, which should not trigger a stress response due to the friendly and encouraging behavior of the panel not inducing a social-evaluative threat despite relatively similar mental demands. Of the previously mentioned neuroendocrine responses, as a direct effect of stress, the two most important stress signaling pathways are the sympathetic nervous system (SNS) and hypothalamic-pituitary-adrenal (HPA) axis [Mil02]. α-amylase is the sensitive biomarker for the activation of the SNS, responsible for the "fight-or-flight" response [Nat09] and the activation

of the HPA axis is assessed by an increase in cortisol [Goo17]. In addition, SNS activity can be characterized by measuring electrophysiological signals, such as electrodermal activity or electrocardiography, from which heart rate and heart rate variability can be derived [Daw16].

Nevertheless, the well-established methods for measuring neuroendocrine and electrophysiological markers, can mean a great deal of effort for the researcher and, in some cases, there is no alternative to invasive methods. If considering the measurement of inflammatory reactions, which are activated as an acute stress reaction [Roh19], this can currently only be measured accurately through the blood, which as an invasive approach may influence natural behavior [Sla15].

Prior studies have demonstrated that encountering acute psychosocial stress has significant impact on an individual's body posture and movement [Abe22], presenting a promising expansion of current markers for acute stress. Incorporating this into stress research offers a non-invasive, holistic approach that may enables early detection of stress responses and could support the development of personalized stress management strategies by recognizing specific patterns and learning strategies to manage them. The gold standard for measuring whole-body movement is a marker-based optical motion capturing (OMC), or an inertial measurement unit (IMU)-based motion capturing approach. However, both techniques are costly and have their drawbacks due to specific sensors that need to be attached, possibly interfering with the participant's natural behavior [Col18] or very time-consuming and tedious calibration processes [Roe09]. A good alternative would therefore be a video-based motion analysis based on established tools such as OpenPose [Cao19] or AlphaPose [Fan23]. This simple and cost-effective method has not yet been widely used in researching stress, probably due to the inaccessibility of these tools to non-technical researchers. A solution for this is offered by the *openTSST* framework, developed at the *MaD Lab*, as an easy-to-use interface to OpenPose as a web application for video-based motion analysis and feature extraction pipeline with a special focus on the analysis of psychosocial stress [Geß23].

The goal of this bachelor's thesis is, to use the *openTSST* framework on video data collected in a study conducted within the EmpkinS collaborative research center, where participants performed the TSST as well as the f-TSST as a control condition on two consecutive days in randomized order. The main focus was on the extraction of movement features and a subsequent statistical and ML-based analysis of these. Thus, previous features were analyzed and new features developed and integrated into the existing *openTSST* framework. This thesis further examined the influence of people performing the tests standing or sitting and whether there were gender differences. Finally, ML techniques were used for classification between the TSST and the f-TSST.

Chapter 2

Related Work

2.1 Influence of Emotional States on Body Posture and Movement

It is possible to perceive and express emotional information via different channels, such as facial expressions, bodily movement, and posture [Gel15]. Thus, human body posture and movements can offer valuable insights into the physical and psychological state of an individual [Bal00; Wal98; Dae12]. In this regard, the following section will mention different studies, starting with facial expressions, followed by research focused on the rest of the body in various scenarios, dynamic movements, and defensive freezing behavior, ended with the current state of research on gender differences in the expression of emotions through movement.

Facial expressions have been widely used for this in the past. For example, Zhan et. al. developed a framework that recognizes the stress-related emotions of anger, fear, and sadness in real time [Zha19]. Others investigated how stress changes facial expressions to assess the potential of facial expressions as a feature for recognizing acute and chronic stress [May19]. Giannakakis et al. used semi-voluntary facial features to recognize stress/anxiety states using ML techniques and features such as eye-related events, mouth activity, and head motion [Gia17].

Atkinson et al. developed dynamic and static whole-body expressions to identify basic emotions like happiness, fear, anger, disgust, and sadness. They demonstrated that these emotions are readily identifiable from body movements, even when using point-light displays (PLDs), reducing the displayed body movement to moving points representing major joints, waist, head, and feet of a person performing an action [Atk04]. Distinguishing similar emotions was also achieved by changes in body movements within dance motions. Significant for the classification of happiness,

sadness, and fear were the frequency of upward arm movement, duration of times the arms were kept close to the body, amount of muscle tension, and duration of times an individual leaned forward. Especially relevant for the distinction of anger were the number of tempo changes as well as directional changes in the face and torso [Boo98]. Another study focusing on dance moves was conducted by Camurri et al. focused on expressive gestures in dance, analyzing how dancers convey emotions like anger, fear, grief, and joy. Thereby considered was the underlying structure of rhythm, flow of the movement, and to what extent limbs were contracted or expanded in relation to the body center [Cam03].

Shahidi et al. contributed to the understanding of body posture under stress, focusing on how mental concentration impacts cervical muscle activity. They found out that a forward head posture significantly increased with mental concentration compared to baseline [Sha13]. Posture changes can also be used together with head movements in pain assessment. According to Werner et al., these tend to be directed downwards or towards the painful side [Wer18].

Vrij et al. explored the impact of public self-consciousness and behavioral control on hand movements in deceptive situations. Their hypothesis suggested that people with higher self-consciousness and better behavioral control would show fewer hand movements when lying. To test this, they conducted a study with 56 participants, each interviewed once truthfully and once deceptively. Their findings highlighted a link between individual personality traits and non-verbal actions during deception, underscoring how internal states affect physical behaviors [Vri97]. Similar research was conducted by Zee et al. who used a motion capture suit to record movements of the whole body to detect deceit. Whether the interviewees were telling the truth or lying could be determined with an accuracy of 74% based on the sum of the joint displacements, whereby liars tend to move around more compared to the control group [Zee19]. This aligns with the study from Kleinsmith and Bianchi-Berthouze, who underscored the significance of body expressions as a channel for affective communication. They emphasized that full-body movements are equally or sometimes more important than facial expressions, reasoning that people consciously attempt to hide their facial expressions and tend to care less about censoring their body movements [Kle13].

Dynamic movements such as walking can also be informative. In a clinical study, Jarchi et al. found that certain neuronal disorders such as attention deficit hyperactivity disorder, bipolar disorder, autism, dementia, depression, Pick's disease, or Parkinson's disease lead to slower body, hand, and foot movements [Jar18]. Stress may also be a decisive factor. According to Nicolas Rohleder, stress leads to the activation of systematic inflammatory processes in the body [Roh19]. Moreover, such inflammatory processes can become noticeable when walking through shorter,

slower, and wider strides, less arm extension, less knee flexion, and a more downward-tilting head [Las20].

As a bodily reaction to acute stress, various studies have identified freezing behavior, an often significant decrease in body movements [Roe17; Bra04]. Freezing is one of the most common defense reactions in animals to protect themselves from predators [Eil05; Löw15]. Zito et al. investigated stress-induced postural motor responses in patients affected by functional movement disorders (FMD). The participants and a healthy control group were exposed to the TSST. In contrast to the FMD patients, the healthy participants showed a reduction in thorax sway over time [Zit19]. Doumas et al. assessed whether similar stress-related changes in postural sway could be observed by using social evaluative threats to induce stress. During an arithmetic task, twelve young adults were given negative feedback about their performance while additionally being watched, which caused the anticipated reduction in body sway [Dou18]. Similar behavior was observed by Roelofs et al. who studied 40 female participants placed on a stabilometric force platform while being exposed to social threats to investigate if they could induce freezing behavior. A notable reduction in the participants' body sway was achieved by angry faces [Roe10]. This study was replicated and extended by Noordewier et al. with prior recording of a baseline of the participants. The results obtained support the basic hypothesis that participants show physiological signs of freezing when looking at angry faces [Noo20]. Further, Hagenaars et al. observed freezing-like responses to unpleasant films [Hag14]. Using IMU technology, Abel found that in 41 participants who were subjected to the TSST, the participants showed defensive freezing behavior based on the movements of the head, hands, chest, and general body movement compared to the f-TSST as a control condition [Abe22]. Using a similar study protocol and IMU data, Richer et al. were able to detect acute stress with a mean accuracy of 73.4% using ML techniques [Ric24].

The influence of gender on the expression of emotions and internal states through body posture and movement does not yet have a clear answer and remains largely unexplored. Additionally, the majority of the studies focus on the differences in perception of emotions rather than the expression. A study by Alaerts et al. used PLDs to display bodily movements like walking, jumping on the spot, wiping a table, drinking from a water bottle, or kicking a ball with the right leg. These movements were carried out in different emotional states, namely happy, sad, angry, and neutral. They found out that females were significantly faster in recognizing the displayed emotions [Ala11]. Another study by Sokolov et al. also used PLDs to portray knocking on a door with different emotional expressions. They, however, found out that gender affected accuracy rather than speed, modulated by the underlying emotions. Males more accurately recognized happy, and women hostile angry and neutral knocking [Sok11]. This partially aligns with the findings from Krüger et

al. who found out that males surpass females in recognition of happy walking and females tend to be more accurate in recognizing angry locomotion [Krü13]. Another study found evidence, that women recognize basic emotions and negative facial expressions far more accurately than male participants who tend to be significantly better at decoding negative body postures [Cha22]. Due to the lack of research on gender differences in expressing, rather than perceiving, emotions and internal states through body posture and movement, the evaluation of gender differences is covered in this thesis.

2.2   Applications of Video-Based Motion Analysis

Several applications, also to answer research questions similar to those outlined above, use video-based motion analysis, which is characterized by a low barrier of entry and has also been further improved by recent advancements in computer vision.

FaceReader (Noldus, Wageningen, the Netherlands) is often used to recognize facial expressions. With the help of deep learning (DL) algorithms, a person's face is recognized using almost 500 keypoints and decoded facial expressions are then classified by artificial neural networks (NN) to obtain information about emotional reactions and an objective assessment of emotions [Nol23]. So, for example, *FaceReader* was used to recognize consumer emotions in graphic styles which provides a preferable basis in relevant fields of design practice and marketing [Yu17]. Terzis et al. evaluated the efficiency of *FaceReader* during a self-assessment test by comparing the instant measurements of *FaceReader* with the estimations from researchers of students' emotions regarding disgust and anger. Results showed an 87% efficacy suggesting a potentially successful integration in an affect recognition system [Ter10].

Sport is a field in which video-based analysis is also used as an indispensable training tool to analyze an athlete's performance to assess the effectiveness of training for instance [Bar08; Wil08], most recently with the help of other technologies such as DL [Ran20]. By adding human pose estimation together with artificial intelligence (AI), a personalized training can be developed for the athlete, to identify certain incorrect postures that should be corrected for improved performance [Wan19; Par22].

Video-based motion analysis has also found use in human gait analysis [Sin18]. Suman and Verlekar explored the classification of spinal deformities such as Kyphosis and Lordosis with 29 individuals simulating these conditions together with a normal gait. Applying a specific NN operating on key body points, they were able to successfully classify these spinal deformities manifesting not only in the gait but in the movement of the entire body [Sum23]. Abe et al.

developed a diagnosis system using human pose estimation from video analysis for Parkinson's disease aiming to facilitate early detection by analyzing arm angles from videos of patients with varying Parkinson's disease conditions [Abe21]. Stenum et al. also used video-based human pose estimation for human gait analysis. They compared spatiotemporal and kinematic gait parameters calculated based on keypoints obtained by the human pose estimation against those from three-dimensional motion capture. The resulting low mean absolute errors demonstrate the potential of accessible video-based analysis in gait research [Ste21]. Boswell et al. took advantage of the fact that the use of video-based methods does not necessarily require a controlled environment and specialized equipment by conducting a nationwide study across 35 US states in which participants performed the five-repetition sit-to-stand test while filming themselves with a phone. A later analysis of the data using human pose estimation revealed that the movement parameters were significantly related to osteoarthritis diagnoses, physical and mental health, Body Mass Index (BMI), age, and ethnicity [Bos23].

Studies that focus on stress and affective emotion recognition have also used video-based motion analysis. Giakoumis et al. conducted an experiment with 21 participants using a custom Stroop color word test as a stress-induction protocol. They introduced activity-related behavioral features for the upper body, like global activity level, activity symmetry, or frequency of specific hand movements from video and accelerometer recordings. Their findings indicated that several behavioral features extracted from video sequences with descriptors like Motion History Images, significantly correlated with self-reported stress [Gia12]. Using two consumer video cameras, Glowinski et al. also focused on upper body movement, particularly head and hand movements, to extract expressive and affective information. They calculated different expressive features like the smoothness/jerkiness, regarding the motion continuity, by calculating the third derivative of movement position. They further calculated the spatial extent using a bounding triangle between the centroids of head and hands, taking the dynamics of the perimeter approximating the space occupied by the extremities from the frontal view. Their results showed that jerkiness related to emotions like fear or despair, whereas continuous and spatially invariable movements portrayed emotions such as anxiety and fear [Glo11]. The paper from Lefter et al. analyzed hand gestures at service-desk interaction scenarios. The gestures were categorized into different classes and based on semantic meaning and modulation (i.e. rhythm, speed, jerk, expansion, and tension). They found out that gesture modulation was a significant indicator of stress with certain gestures, such as sudden, tense, or repetitive movements being particularly indicative [Lef16]. Aigrain et al. used a Kinect device to capture skeleton and video data during a self-designed, evaluated, and time-constrained mental arithmetic test. The key features extracted included the Quantity

of Movement (QoM) calculated by the sum of joint displacements between two frames, high activity periods, and posture changes by using the peaks of the QoM computed for each frame. Additionally, they detected self-touching using a threshold for the distance between the hands or hands and head region. Using a ML model trained on these features, they were able to detect stress with an accuracy of 77% [Aig15]. In a follow-up study, Aigrain et al. again used a Kinect for video and skeleton data for stress detection. They once more computed the QoM but in two forms: IQoM as the number of pixels that change between two consecutive frames and the SQoM from displacements of the skeleton joints as well as self-touching. Utilizing peaks in the IQoM signal to detect periods of high body activity which could characterize an increasing uncomfortability. They further used the pixel difference of the first and last frame of such a period to detect a change in posture. They suggested that behavioral in combination with physiological features could enhance automatic stress detection [Aig18].

Chapter 3

Methods

3.1 Data Acquisition

To investigate the effects of acute psychosocial stress on body movements and posture, a study was conducted at the *MaD Lab* from December 2022 to December 2023. Participants were exposed to the TSST and the f-TSST on two consecutive days. The condition order was swapped after each pair of days to obtain a balanced data set. Both tests were either performed standing or sitting, which was randomly assigned.

3.1.1 Study Population

In total, 101 participants (58 females and 43 males) were recruited for the study. Information about gender, position during the (f-)TSST, and condition order of all participants can be taken from Table 3.1, demographic and anthropometric data from Table 3.3.

Table 3.1: Gender, position, and condition order overview of entire study population.

Condition order	Female		Male		Total
	Sitting	**Standing**	**Sitting**	**Standing**	
f-TSST first	19	13	11	10	53
TSST first	13	13	7	15	48
Total	32	26	18	25	101

Due to incomplete data, 18 participants had to be omitted from the data processing. The final data set consisted of 48 female and 35 male participants. Table 3.2 provides an overview of their condition order and position.

Table 3.2: Gender, position, and condition order overview of used study population.

Condition order	Female		Male		Total
	Sitting	**Standing**	**Sitting**	**Standing**	
f-TSST first	14	11	9	9	43
TSST first	11	12	6	11	40
Total	25	23	15	20	83

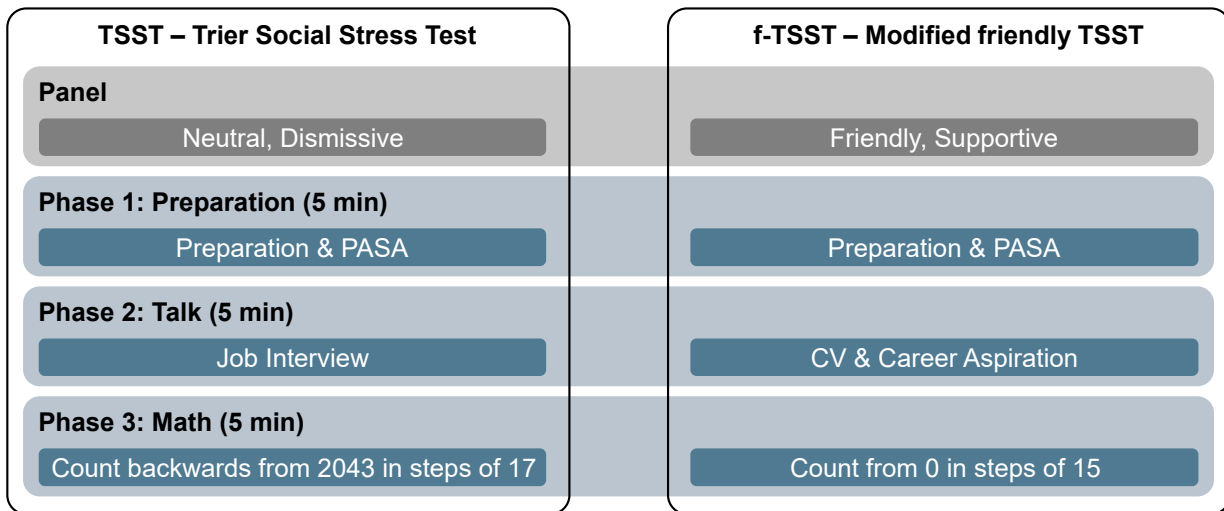**Table 3.3:** Demographic and anthropometric data of all participants; Mean $\pm$ Standard deviation (SD).

	Age [years]	**Height** [cm]	**Weight** [kg]	**BMI** [kg/m^2]
Female	22.04 ± 3.72	168.52 ± 6.91	62.66 ± 7.57	22.04 ± 2.26
Male	22.33 ± 2.88	183.07 ± 6.88	78.80 ± 11.49	23.55 ± 3.46
All	22.16 ± 3.36	174.71 ± 9.97	69.53 ± 12.35	22.68 ± 2.91

Participants were recruited using electronic flyers via social media platforms as well as printed flyers distributed throughout university buildings or in person in the canteen or library. Ineligible for the study were people under 18 or over 50 years old, not native German speakers, with a BMI below 18 or above 30, suffering from physical or mental health conditions, were taking any medications, smoked, used drugs, were obese, or had previously taken part in a similar stress test. Interested individuals had to complete a digital screening beforehand and were only allowed to participate if they met these conditions. Psychology master students were also excluded, as there is a high probability that they are already familiar with the (f-)TSST. As a reward for their participation, individuals could choose between receiving 50 Euros or 5 *Versuchspersonenstunden* (for psychology bachelor students).

3.1.2 Acute Stress Induction

To induce acute psychosocial stress in the participants, the TSST was used, which is considered the gold standard in a laboratory setting [Kir93]. The f-TSST was used as a control condition, which should not trigger a stress response despite relatively similar mental demands [Wie13]. Although the protocol of the f-TSST was slightly modified to achieve a better comparability with the TSST. The main differences between the TSST and the f-TSST can be seen in Figure 3.1. Deviating from the protocols, the panel consisted only of women from about halfway through the study due to the lack of male staff.

TSST – Trier Social Stress Test		f-TSST – Modified friendly TSST
Panel		
Neutral, Dismissive		Friendly, Supportive
Phase 1: Preparation (5 min)		
Preparation & PASA		Preparation & PASA
Phase 2: Talk (5 min)		
Job Interview		CV & Career Aspiration
Phase 3: Math (5 min)		
Count backwards from 2043 in steps of 17		Count from 0 in steps of 15

Figure 3.1: Protocol comparison between the TSST and f-TSST.

TSST

The panel for the TSST consisted of two people the participant did not know, both wearing white lab coats intended to reinforce a more serious laboratory environment [Wie13]. The active panel member, who sat on the left from the perspective of the participant, took over the active part of the experiment, i.e., the interaction with the candidate. They received explicit directives to maintain a neutral demeanor, minimizing their responses to the participant's behavior. The protocol consisted of three distinct phases, each lasting five minutes: Preparation, Talk, and Math, outlined in 3.1. After the test director explained the protocol and left the room, the first phase began. The briefing included that participants were to imagine a job interview setting and that the panel would decide about employment in their dream job, which they told the test director beforehand. Emphasis was placed on the participant talking about personal attributes, which should justify suitability for the position, rather than professional competencies. A three-minute interval was allocated for note-taking, aimed at structuring their talk. This was followed by a two-minute session dedicated to the completion of the Primary Appraisal Secondary Appraisal (PASA) questionnaire [Gaa09], to asses cognitive appraisal processes in a stressful situation [Car16]. Participants were, however, not allowed to bring their notes to the subsequent talk phase.

Afterward, a dual-camera setup, detailed in Section 3.1.3, started recording, and participants were instructed to start with their speech. Observing the beginning of the video recording contributes to the social evaluative component of the stress response and is therefore an important element of the TSST [Lab19]. The expectation was to maintain a continuous monologue and the panel only interrupted if the participant deviated from talking about personal attributes, silences

surpassing 20 seconds, or if the participant no longer maintained eye contact with the active panel member. The final phase was an arithmetic challenge, in which the participant should count back from 2043 in steps of 17. In case of an error, the panel intervened, prompting to restart from 2043.

f-TSST

Mirroring the framework of the TSST, the f-TSST unfolded before a duo of panelists. The f-TSST was designed to evoke minimal stress while preserving an ambiance analogous to the TSST. In doing so, the panelists abstained from wearing lab coats, to support the setting of a more casual environment, and exhibited a demeanor that was not just non-neutral but overtly friendly and encouraging throughout the protocol. Additionally, the active panel member left the room during the preparation phase to further relax the participant [Wie13].

The talk segment of the f-TSST deviated from the conventional TSST format, pivoting towards a dialogue centered on the participant's Curriculum Vitae and career aspirations, as opposed to the high-pressure milieu of a job interview. Notably, the original f-TSST protocol does not include a computational component. Therefore, the numerical task from the placebo-TSST [Het09] — another variant of the TSST conceptualized as a stress-diminished control condition — got integrated for consistency and to maintain a low-stress environment. During this segment, participants had to numerically increment in steps of 15, starting from zero. Any computational errors were addressed with sympathy, and participants being gently informed of the mistake and encouraged to proceed from the last correct number.

3.1.3   Test Procedure

Pre-Test Phase

After a participant arrived at the laboratory, they were guided to the preparation room where they first signed a declaration of consent. Following was a brief explanation of the timeline by the study leader and the participant provided the first out of eight saliva samples (S_0). An overview of the saliva sampling times can be found in Table 3.4.

Table 3.4: Saliva sampling times relative to the (f-)TSST start.

Relative time [min]	-40	-1	0-15	$+16$	$+25$	$+35$	$+45$	$+60$	$+75$
Saliva samples	S_0	S_1	*(f-)TSST*	S_2	S_3	S_4	S_5	S_6	S_7

To minimize the effects caused by interindividual differences in energy availability, participants were provided 200ml of grape juice, substituted with sugar water for fructose-intolerant participants [Zän20]. Females additionally gave a passive drool sample on the second day to determine progesterone levels to detect menstrual cycle-related changes in the cortisol response to acute stress [Ham20]. A body scale was used to determine the participant's body weight, body fat, and muscle percentage.

(f-)TSST

All participants were filmed by two cameras during the talk and math phase of the (f-)TSST. An RGB camera (Sony SRG-300H, Minato, Japan) filmed the head and an RGB-D camera (Microsoft Azure Kinect, Redmond, WA) filmed the entire body. The RGB-D camera was replaced by a cell phone (Google Pixel 7A, Foxconn, Tucheng, Taiwan) close to the beginning of the second half of the study. During the (f-)TSST, the times of individual phases of the protocol (3.1) were tracked with a mobile application (aTimeLogger - Time Tracker, BGCI)[1].

Post-Test Phase

After the (f-)TSST, participants were guided back to the preparation room providing the next saliva sample (S_2: about 15 min after the (f-)TSST start). The remaining saliva samples were taken according to the relative times provided in Table 3.4.

3.1.4 Video Data

As the *openTSST* platform only accepts videos in the MP4 file format, the MKV output files from the Kinect were converted into MP4 files with H.264 encoding. The used cell phone saved the recordings as MP4 files, which were compressed before uploading.

openTSST Output

This thesis only used the full-body videos, uploaded in a resolution of $1920{\times}1080$ for the Kinect, and $1080{\times}1920$ for the phone, respectively, to the *openTSST* web application. The output was a Comma-separated values (CSV) file, with one row for each frame of the video and three columns (x, y, c) for each key body part, representing the x, y coordinates, and a confidence value extracted by the *openTSST* framework [Geß23] utilizing OpenPose [Cao19]. An overview of the key body parts extracted by OpenPose can be found in Figure 3.2.

---

[1]https://play.google.com/store/apps/details?id=com.aloggers.atimeloggerapp (visited on 03/02/2024)

No.	Keypoint
0	Nose
1	Neck
2	Right Shoulder
3	Right Elbow
4	Right Wrist
5	Left Shoulder
6	Left Elbow
7	Left Wrist
8	Mid Hip
9	Right Hip
10	Right Knee
11	Right Ankle
12	Left Hip
13	Left Knee
14	Left Ankle
15	Right Eye
16	Left Eye
17	Right Ear
18	Left Ear
19	Left Big Toe
20	Left Small Toe
21	Left Heel
22	Right Big Toe
23	Right Small Toe
24	Right Heel

Figure 3.2: OpenPose BODY_25 body part mapping.

Data Cleaning

The CSV file received from *openTSST*, however, included a larger time frame of the video, which was actually of interest. This is because the video recording started before the (f-)TSST and only stopped after a panel member had unplugged all the participant's cables from various measuring instruments and the participant had left the room. A clapperboard was used as the start and end point for the data, which was closed in front of the camera before the talk and after the math phase of the (f-)TSST. This reduced the additional data that was not part of the actual test to a few seconds, in which the passive panel member briefly came in front of the camera, closed the clapperboard, and sat down again. Therefore, the start and end frames, defined by the frame in

which the clapperboard was closed, were manually extracted for all videos individually using DaVinci Resolve 18 (Blackmagic Design, Port Melbourne, Australia). To analyze the individual phases of the (f-)TSST, the start frame of the talk phase was extracted, which was determined manually based on the vocal prompt from the panel that the participant should start their talk. However, this was only possible for the cell phone videos, as no sound was available for the Kinect recordings. The start of the math part and the end of the (f-)TSST were then calculated using the times logged by the panel. Afterward, all CSV files from *openTSST* got trimmed to only include the key body parts information from the extracted start to end frame of the corresponding video.

Data Normalization

All data was normalized based on body height and considering whether the participants performed the (f-)TSST standing or sitting. This was essential to compensate for differences in the orientation of the camera between tests and participants to ensure that the results obtained were comparable. The body height was calculated as the 95th percentile of the vertical distance between two keypoints y_{upper} and y_{lower} for the entire data sequence (equation 3.1). While the "Nose" keypoint (fig 3.2) was always used for y_{upper}, y_{lower} depended on whether the participant performed the (f-)TSST in a standing or sitting position. Equation 3.2 was used in the standing case for each frame i. The average was used because the camera was not filming from the front, but from the participant's perspective slightly to the right. As a result, the "Right Heel" keypoint had a larger y-value with a symmetrical stance, which was compensated for as best as possible. For the seated case, the "Mid Hip" keypoint was used for y_{lower} and, assuming that the difference between upper body and leg length does not substantially vary, normalized only for the upper body. This had to be done because the sitting position varied greatly between the participants. Some participants sat with their legs stretched out, had their feet firmly on the floor or sat with one leg crossed over the other.

$$height = quantile(y_{\text{lower}} - y_{\text{upper}}, q = 0.95) \tag{3.1}$$

$$y_{\text{lower},i} = \frac{1}{2}(y_{\text{LeftHeel},i} + y_{\text{RightHeel},i}) \tag{3.2}$$

Additional Preprocessing

Further preprocessing steps were analog to [Geß23], which will be briefly described in the following. Before normalizing the data, as outlined above, OpenPose's occasional failures in pose detection were addressed by using linear interpolation for missing keypoint estimations and discarding gaps

over half a second. Furthermore, to minimize the impact of high-frequency, low-magnitude noise, a 6 Hz, fifth-order, zero-lag, low-pass Butterworth filter was applied to the data.

The position of each body part relative to the neck was determined by calculating the difference between the coordinates of the neck and the opposed body part. The same method was used for the position of each wrist to its corresponding elbow.

Finally, velocities in the x- and y-dimensions, as well as the 2-dimensional velocity were computed. For the x and y components, the Euclidean norm was applied to the respective differences in the x and y coordinates of the position. Similar computations were made for the 2-dimensional velocity which was additionally divided by the elapsed time, resulting in the velocity measured in units of pixels per frame.

3.2   Endocrinological Features

To assess the activity of the HPA axis and confirm the anticipated stress reaction induced by the TSST, four saliva features were calculated from the raw cortisol values obtained by the saliva samples (S_0 - S_7). This involved the maximum cortisol increase (Δc_{max}), the slope from S_1 to S_4 (m_{S1S4}), and, termed by Pruessner et al., the 'Area under the curve with respect to ground' (AUC_g) as well as the 'Area under the curve with respect to increase' (AUC_i) [Pru03]. The first saliva sample (S_0) was excluded from the analysis, as the main purpose of it was for baseline comparisons and a potential retrospective exclusion of participants. For the remaining samples (S_1 - S_7), the features were calculated as follows, where t_i denotes the time of the measurement and S_i is the corresponding cortisol level.

The maximum increase in cortisol (Δc_{max}), expressed as the difference between the peak cortisol level after the TSST and the cortisol level S_1, measured right before the TSST:

$$\Delta c_{max} = \max\{S_2, ..., S_7\} - S_1 \tag{3.3}$$

The slope m_{S1S4} between S_1 and S_4 was calculated as:

$$m_{S1S4} = \frac{S_4 - S_1}{t_4 - t_1} \tag{3.4}$$

Furthermore, the AUC_g, quantifying the 'Area under the curve with respect to ground' was computed as:

$$AUC_g = \sum_{i=1}^{6} \frac{(S_{i+1} + S_i) \cdot (t_{i+1} - t_i)}{2} \tag{3.5}$$

Finally, the equation for AUC_i, representing the 'Area under the curve with respect to increase' is:

$$AUC_i = \sum_{i=1}^{6} \frac{(S_{i+1} + S_i) \cdot (t_{i+1} - t_i)}{2} - S_1 \cdot (t_7 - t_1) \tag{3.6}$$

3.3 Motion Feature Calculation

After the data preprocessing, various features were computed, mostly similar to previous work [Abe22; Ric24]. These features were calculated for the individual body parts. To quantify movements of composite body regions, some body parts were additionally grouped according to Table 3.5. The calculated features can be divided into two categories, generic and expert features. *Generic features*, accessible without specialized domain knowledge, included fundamental statistical metrics such as mean and SD in addition to signal characteristics like entropy. *Expert features*, conversely, rely on pre-existing expertise and are tailored to delineate movement patterns identified in prior research or observations during data collection. The calculated features are listed in Table 3.6 for the generic, and in Table 3.7 for the expert features, respectively. The metrics for the expert features are detailed in B.1.

Table 3.5: Definition of body part groups; {L/R} denotes the left and right side.

Group	Body Parts
Trunk	{L/R} Hip, {L/R} Shoulder, Neck
Upper Extremities	{L/R} Shoulder, {L/R} Elbow, {L/R} Wrist
Lower Extremities	{L/R} Knee, {L/R} Ankle, {L/R} BigToe, {L/R} SmallToe, {L/R} Heel
Total Body	All body parts

Static Periods

To measure anticipated freezing behavior, *static periods* were identified in $0.5\,\text{s}$ windows with a 50% overlap. A window was considered static if its total variance fell below a certain threshold

Table 3.6: Overview of computed generic features.

Name	Abbreviation
Mean	mean
SD	std
Entropy	entropy
Absolute Energy	abs_energy
Mean Crossing	mean_crossing
Zero Crossing	zero_crossing
Fast Fourier transform (FFT) Aggregated Centroid	fft_aggregated_centroid
FFT Aggregated Kurtosis	fft_aggregated_kurtosis
FFT Aggregated Skew	fft_aggregated_skew
FFT Aggregated Variance	fft_aggregated_variance

based on the observed body part. The thresholds for the velocity norm can be taken from B.2 and for the velocity norm relative to the neck from B.3. In addition, for the left and right wrist, the expert features mentioned in Table 3.7 were further calculated relative to the corresponding elbow with a threshold of 2×10^{-7}. All the thresholds were determined iteratively by manually comparing the computed feature value to the actual video data.

Euclidean Distance

Observations indicated that participants experiencing acute stress tended to bring their hands closer together, touch their heads more often, and adopt a tenser posture. Consequently, the Euclidean distance, as a simple and for this purpose previously successfully used method [Car06; Gia12], between the left and right wrist, as well as between the wrists and nose keypoint, was computed. Additionally to the mean and SD of that distance throughout the (f-)TSST, frames in which a pair of these body parts were close together were counted. This was achieved by applying a threshold on the Euclidean distance calculated for each frame. Due to the different normalization techniques, based on whether participants performed the (f-)TSST standing or sitting, different thresholds were applied. For standing participants, a threshold of 0.11 was used between the wrists and 0.095 for the {L/R} wrist and the nose. For the seated position 0.095 between the wrists and 0.35 between the {L/R} wrist and the nose. These thresholds were determined by manually searching for videos where the participant touched their nose or had their hands very close together, indicating the minimum Euclidean distance throughout the video. Followed was adding a buffer of 25% for touching the head to also capture head scratching, touching chin, etc. For bringing their hands closer together, a buffer of 40% was used. The higher buffer for the hands was because the wrists

were the representative keypoints for hands and touching fingers should also be captured. The thresholds were checked by manually counting the frames and comparing them to the computed results for a small subset of the data.

Table 3.7: Expert features overview.

| Name	Abbreviation	Channels	Metrics
Static Periods	stat_periods	vel_norm vel_norm_rel2neck	count_per_min max_duration_sec mean_duration_sec longer_than_3sec std_duration_sec ratio_percent
Euclidean Distance	eucl_dist	pos_norm	mean std frames_below_threshold

3.4 Evaluation

3.4.1 Statistics

The Shapiro-Wilk test was used to check the data for normal distribution at the beginning to determine the type of subsequent statistical test [Pea08]. However, once this showed nonconformity for the majority of features, further testing was carried out with a non-parametric test. The paried Wilcoxon signed-rank test [Wil45] was performed for all features, as a non-parametric equivalent of the paired t-test [Dam23], with the condition (TSST or f-TSST) as the within variable. This was possible because there was full data for both the f-TSST and the TSST for each participant included in the statistical analysis. All statistical computations were performed using the Python package *biopsykit* [Ric21] based on *pingouin* [Val18]. The significance level was set at $\alpha = 0.05$, and *t*-test effect sizes were reported as Hedge's g. Despite the highly explorative character of the study, an attempt was made to correct for the multiple comparisons problem using Bonferroni corrections across all tests [Arm14]. All figures and tables utilise the following notation to denote statistical significance: *$p < 0.05$,** $p < 0.01$,*** $p < 0.001$.

The motion features described in 3.3 were used for all statistical analyses. To assess the influence of acute psychosocial stress on body posture and movements, statistically significant

features were be reported. In addition to these, or should there be none, other noticeable features or characteristics that have proven to be conclusive in studies mentioned in chapter 2 were evaluated.

3.4.2 Classification

To distinguish between the TSST and the f-TSST in standing position, a ML model was trained on the calculated motion features. Only the standing participants were considered, as only for these was it possible to differentiate between the conditions. The classification pipeline used for this is shown in Figure 3.3.
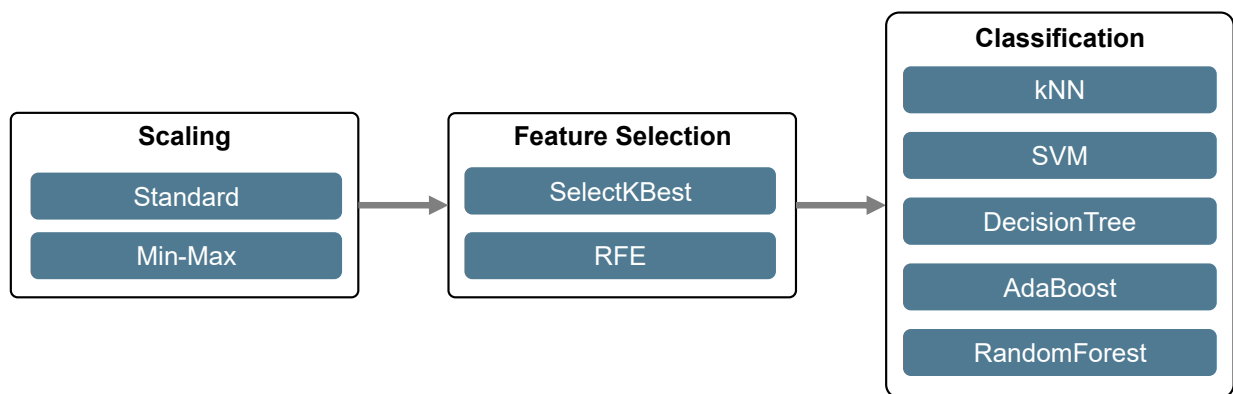
Figure 3.3: Trained classification pipeline.

A total of five different models were trained for classification, namely *k-nearest neighbors (kNN)*, *Support vector machine (SVM)*, *DecisionTree*, *Adaptive Boosting (AdaBoost)*, and *RandomForest*. Using a five-fold cross-validation (CV), they were evaluated according to the mean test accuracy. With each iteration of the CV, the hyperparameters of the feature selection and classification were optimized using grid search, and for *RandomForest* random search with 100 iterations. During each segment of the cross-validation process to optimize the hyperparameters, the features were first scaled by either *StandardScaler* or *MinMaxScaler*. The *StandardScaler* normalizes the features by adjusting their distributions so that they have a mean of 0 and a SD of 1, using z-score normalization. The *MinMaxScaler*, on the other hand, adjusts the features so they fall within a range of 0 to 1. After scaling, the dimensionality of the feature space was minimized using either *SelectKBest* or *recursive feature elimination (RFE)*. *SelectKBest* selects the top *k* features based on the highest analysis of variance (ANOVA) F-score, effectively reducing the number of features. In the case of RFE, an SVM estimator is used to determine the importance of each feature. Subsequently, the features deemed least important are gradually eliminated until

the target number of features is reached. The above-outlined CV approach has been successfully utilized in the past [Abe19; Abe22]. The used hyperparameter grid is shown in Table 3.8.

Table 3.8: Used hyperparameter grid; [1] RandomizedSearch was used for RandomForest.

Feature Selection	Hyperparameter	Values
SelectKBest	k	2 to 5; steps of 1
RFE	n	2 to 10; steps of 2

Classifier/Regressor	Hyperparameter	Values
kNN	k	2 to 20; steps of 2
	weights	uniform, distance
DecisionTree	criterion	gini, entropy
	depth	2, 4
SVM	kernel	linear
	C	$10^{-2}, 10^{-1}, 10^0, 10^1, 10^2, 10^3, 10^4$
AdaBoost	base_estimator	DecisionTree
	n_estimators	10 to 500; steps of 20
	learning_rate	0.01 to 1; steps of 0.1
RandomForest [1]	bootstrap	True, False
	max_depth	5 to 50; steps of 5
	max_features	auto, sqrt
	min_samples_leaf	1 to 10; steps of 1
	min samples_split	2 to 20; steps of 1
	n_estimators	10 to 500; steps of 10

Chapter 4

Results & Discussion

4.1 Endocrinological Measures

As the laboratory had not yet finished analyzing the saliva samples at the time of writing this thesis, only the cortisol data from the first 45 participants was used.

The cortisol increase peaked with sample S_3, 10 min after the end of the (f-)TSST as shown in Figure 4.1. Compared to the f-TSST, the average maximum value of the TSST was approximately 66% higher. A substantial increase of 157% in the TSST and just under 42% in the f-TSST occurred for S_3 relative to the baseline measure S_1, which was taken immediately before the (f-)TSST.
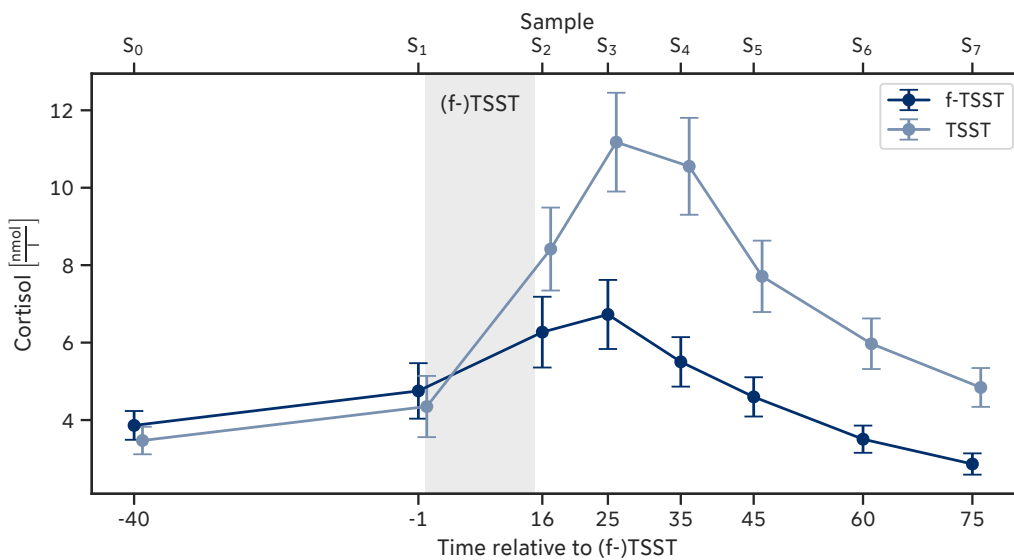
Figure 4.1: Cortisol response; Mean $\pm$ Standard error (SE).

All of the derived cortisol features, shown in Figure 4.2, revealed a significant difference between the TSST and the f-TSST. A list of the statistical test results can be taken from Table 4.1. The largest effect sizes were found for m_{S1S4} with $g = 0.809$ (mean increase of $0.15\,\mathrm{nmol\,L^{-1}}$) and Δc_{max} with $g = 1.024$ (mean increase of $5.13\,\mathrm{nmol\,L^{-1}}$). The outcomes for the endocrinological responses were consistent with previous findings [Abe22; Wie13; All14].
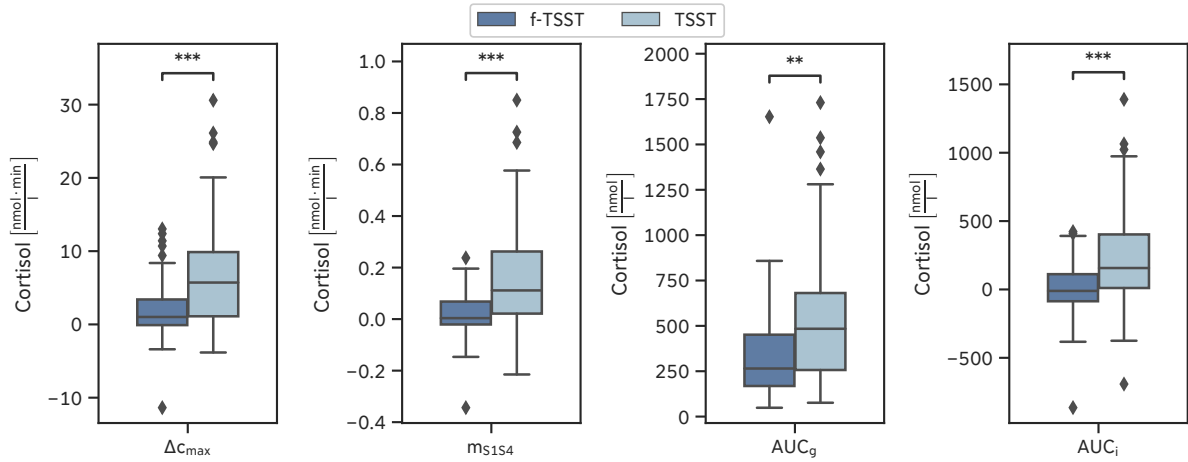
Figure 4.2: Calculated cortisol features; Mean $\pm$ SE.

Table 4.1: Results of statistical cortisol feature analysis.

Feature	T	df	p	Hedges' g
AUC_g	3.097	37	0.004**	0.556
AUC_i	3.766	37	<0.001***	0.710
Δc_{max}	3.979	39	<0.001***	0.746
m_{S1S4}	3.969	38	<0.001***	0.809

No major differences were found when analyzing the cortisol response according to the position in which the (f-)TSST was performed, as can be seen in Figure 4.3. These results indicate that the TSST successfully triggered stress in the participants, regardless of whether the participants performed the (f-)TSST while standing or sitting.
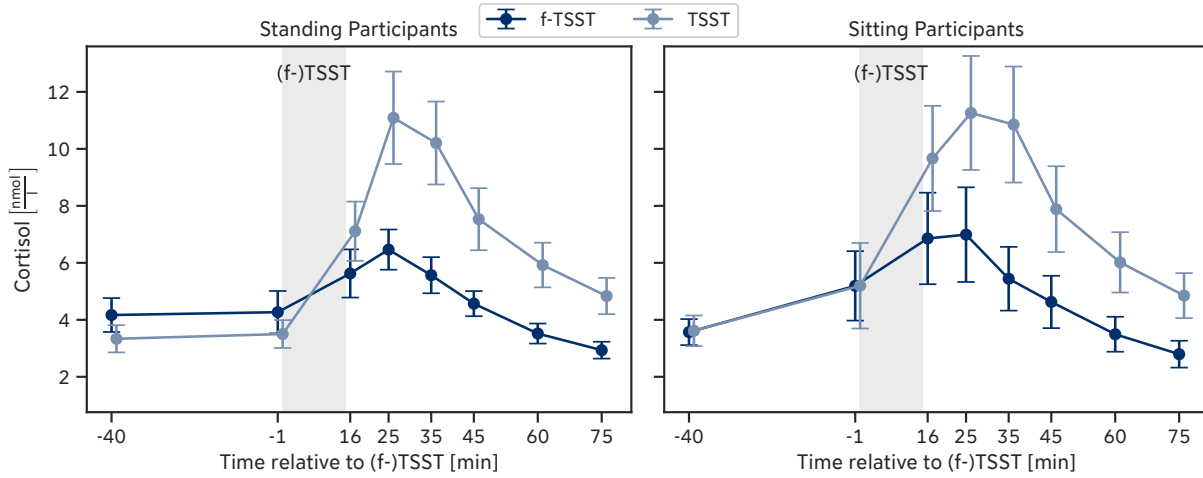
Figure 4.3: Cortisol response separated by position; Mean $\pm$ SE.

## 4.2 Body Posture & Movement Feature Evaluation

4.2.1 (f-)TSST Features In Standing Position

A total of 258 features were computed, of which 8 were statistically significant. These included 2 generic and 6 expert features.

Generic Features

The statistically significant generic features are shown in Figure 4.4. Similar to [Abe22], the generic features showed a reduced head movement during the TSST compared to the f-TSST, represented by the nose keypoint. Looking at mean velocity, the head generally moved 14% less during the stressful situation ($4.53 \times 10^{-4} \pm 1.36 \times 10^{-4}$ vs. $5.27 \times 10^{-4} \pm 1.38 \times 10^{-4}$) and almost 12% less relative to the neck ($5.76 \times 10^{-4} \pm 1.44 \times 10^{-4}$ vs. $6.51 \times 10^{-4} \pm 1.53 \times 10^{-4}$), which could indicate a more tense posture in the cervical region. This would partly align with the findings of Shahidi et al., although participants were sitting during the stressful situation [Sha13].

In contrast to the mentioned studies [Dou18; Roe10; Zit19], no significant reduction in postural sway was observed. The trunk was used as the representative group, which, according to Table 3.5, is made up of the keypoints on the hip, shoulders, and neck. Features that would show such a behavior can be seen in Figure 4.5. The mean velocity was only reduced by 3% during the TSST compared to the f-TSST ($8.4 \times 10^{-4} \pm 2.22 \times 10^{-4}$ vs. $8.69 \times 10^{-4} \pm 2.09 \times 10^{-4}$). A detailed evaluation of all the generic features can be found in Table B.4.
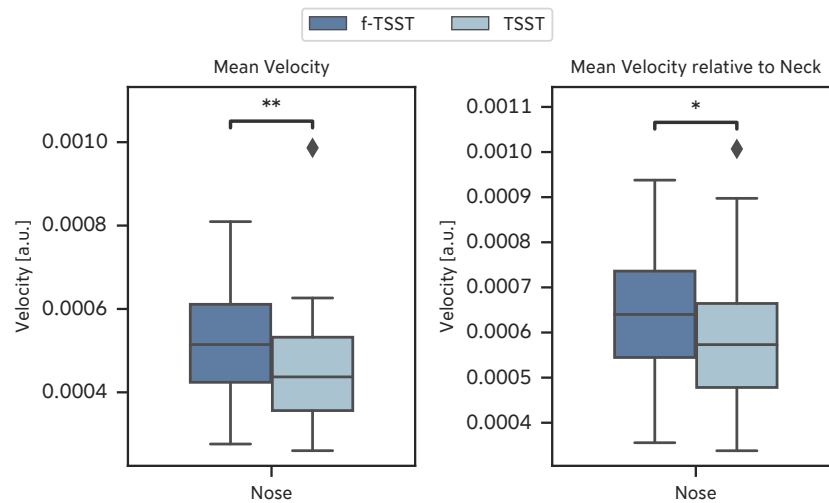
Figure 4.4: Statistically significant generic features; (f-)TSST standing.
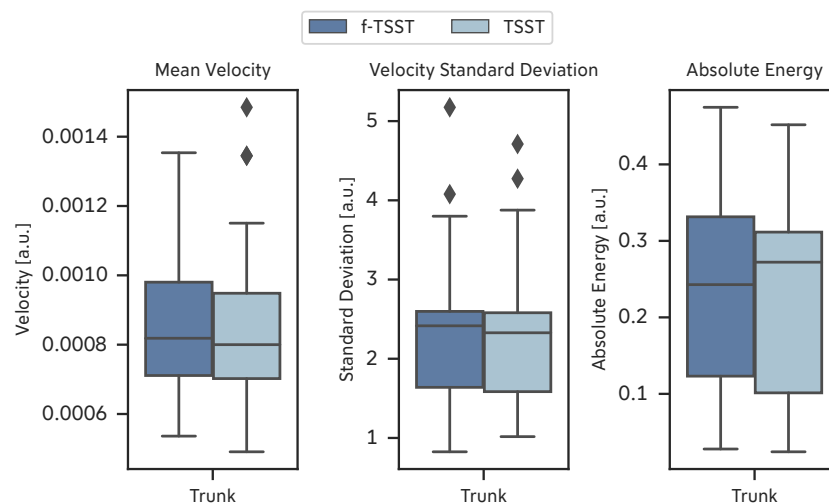
Figure 4.5: Generic features characterizing postural sway; (f-)TSST standing.

Expert Features

The *static periods* showed a significant difference for the head. In Figure 4.6, the features concerning only the nose are displayed. During the TSST, static periods occurred far more frequently each minute. There were, on average, around 19% more static periods during the TSST compared to the f-TSST (32 ± 8 vs. 27 ± 7) in one minute. Additionally, there were 19% more static periods lasting for more than 3 seconds while being exposed to acute psychosocial stress (228 ± 54 vs. 191 ± 53). Analyzing the mean time of the static periods relative to the total length of the (f-)TSST, there was an increase of 33% throughout the TSST compared to the baseline ($16\% \pm 5\%$ vs. $12\% \pm 5\%$).
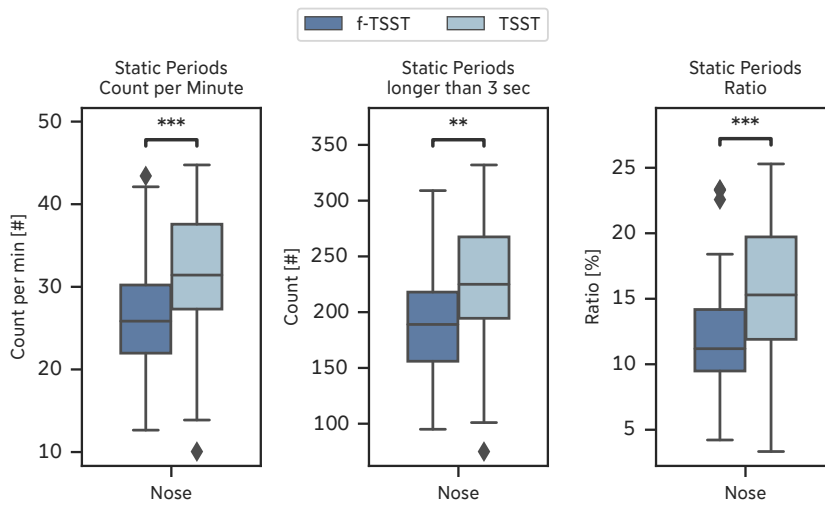
Figure 4.6: Statistically significant expert features for the nose; (f-)TSST standing.

Even more notable results were found when observing the nose relative to the neck (Figure 4.7). Static periods were around 24% more frequent each minute while stressed (26 ± 8 vs. 21 ± 7). Furthermore, there was a mean increase of 26% in static periods longer than 3 seconds, as well as 25% more total static time during the TSST in comparison to the f-TSST. This would further support the conclusion that stressful situations may lead to increased muscle tension in the neck and shoulder area. It has also been shown in the past that stress generally causes increased muscle activity in these areas of the body [Wij10; Nim12]. Decreased movement was also found for the wrists relative to their corresponding elbow which can be seen in Figure A.1.

The computed *Euclidean distance* metrics did not provide any statistically significant results. Especially the attempt to recognize self-touching did not lead to any meaningful findings. Figure 4.8 shows the remaining Euclidean distance features regarding the wrists and nose. The average distance between the wrists was 11% less for the TSST, supporting the observed behavior that the participants tended to keep their hands closer together while being exposed to acute psychosocial stress. There was also an increased SD for the wrists as well as relative to the nose. This elevated variability in movements may indicate more jerky and less smooth motions, and relative to the nose, potentially be reflective of behaviors such as frequently touching the head region. Utilizing the smoothness/jerkiness of movements [Glo11; Lef16] or self-touching [Aig15; Aig18] were used as meaningful features in previous stress reaction studies. A comprehensive overview of all calculated expert features can be found in Table B.5.

The difference in motion and posture features observed during the TSST compared to the f-TSST, concerning less movement or a more tense posture, are characteristic for defensive freezing
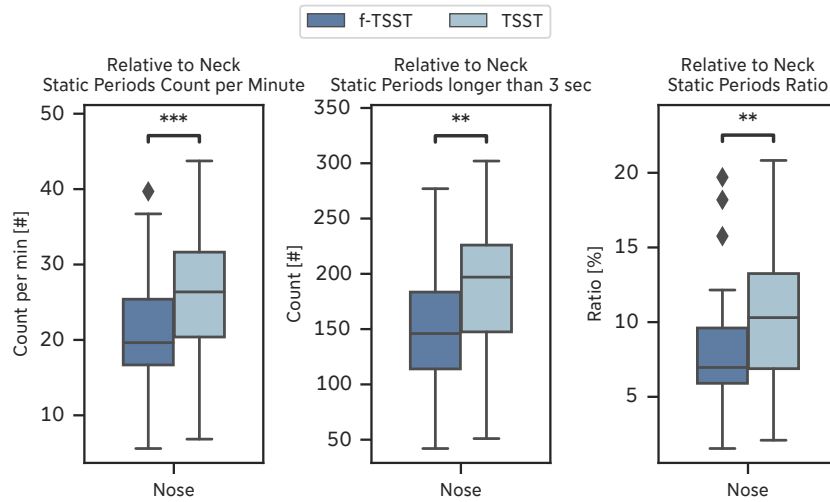
Figure 4.7: Statistically significant expert features for the nose relative to the neck; (f-)TSST standing.
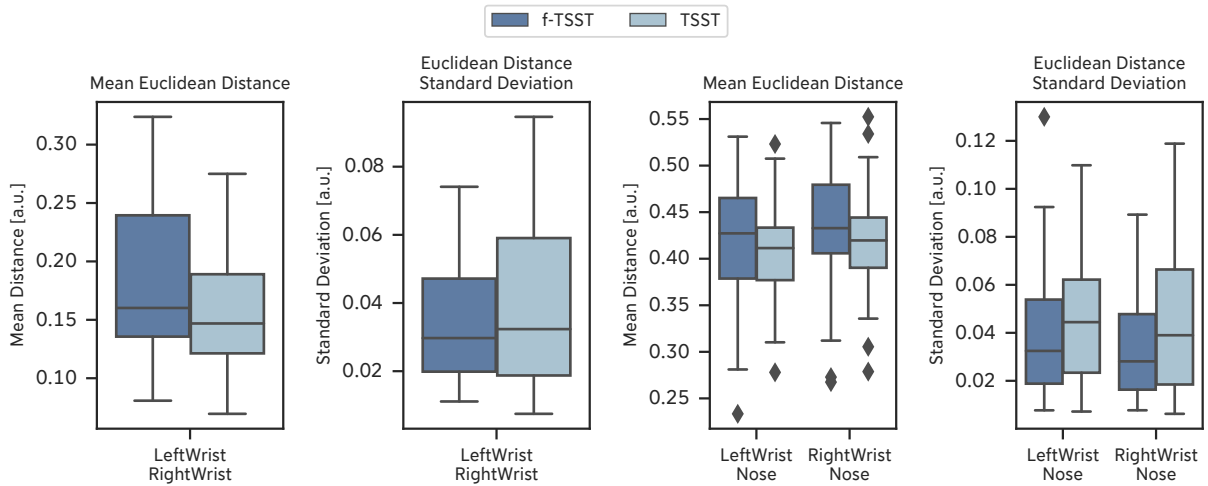
Figure 4.8: Euclidean distance features; (f-)TSST standing.

behavior [Roe17; Bra04] and especially the reduced head movement seemed to be a distinct marker for acute psychosocial stress. Due to the saliva features (4.1) confirming successfully induced stress during the TSST and the statistical significance of the features regarding less or static movement, it would suggest that defensive freezing behavior is a promising indicator for an acute stress reaction.

Condition order

An additional statistical analysis was carried out, which, in addition to the procedure described in 3.4.1, also included the condition order as a between variable. This resulted in p > 0.999 for all features indicating that it did not matter, whether the TSST or f-TSST was performed first.

4.2.2   (f-)TSST Features In Sitting Position

A total of 288 features were computed from which none showed statistical significance with the methods used in this thesis.

Generic Features

The previously descriptive generic features for the (f-)TSST are illustrated in Figure 4.9. During the TSST, there was again a reduction in head movement, but in direct comparison with the f-TSST, this was noticeably less.
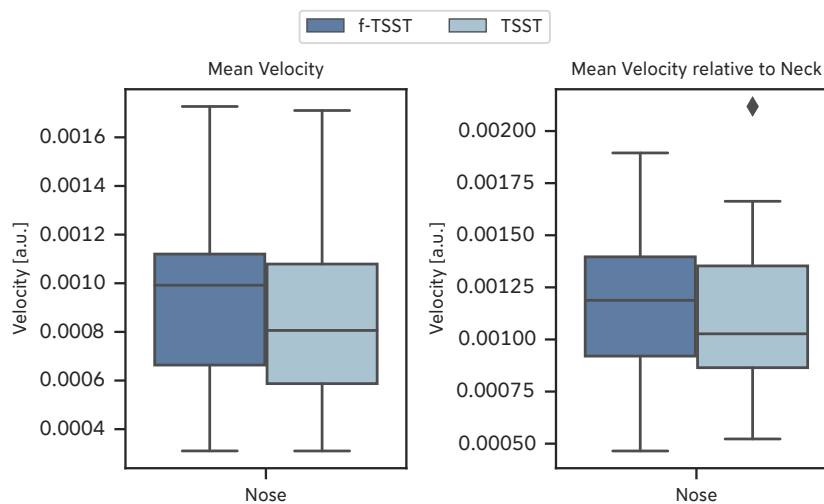
Figure 4.9: Generic features for the nose; (f-)TSST sitting.

Expert Features

Similar to the standing position, there were more static periods during the TSST. Looking at the nose keypoint, this behavior accounted for an average of 16% more of the total length of the recording than during the f-TSST, which can be seen in Figure A.2 (23.4% $\pm$ 8.2% vs.

$20.2\% \pm 7.7\%$). When viewed relative to the neck, there was also a reduction in movement during the stressed condition, but the differences were all less noticeable, as shown in Figure A.3.

An attempt was made to represent leg-shaking in a feature for the seated variant. In addition to a disease-related trigger such as Restless Leg Syndrome or Attention Deficit Hyperactivity Disorder [Was05; All03], it can also be triggered by experiencing anxiousness or agitation [All03]. After examining the static periods of the two knees (Figure 4.10), no clear result was apparent. Both were not showing fewer static periods during the TSST despite the successfully induced stress. However, the static periods of the knees relative to the corresponding big toe, which should remain relatively still when bouncing with the knees, would support the observation. This was quantified by more static periods throughout the recording of the baseline which is displayed in Figure 4.11. Three participants had to be excluded from the analysis as the camera was inaccurately placed, and the feet were not in the frame.
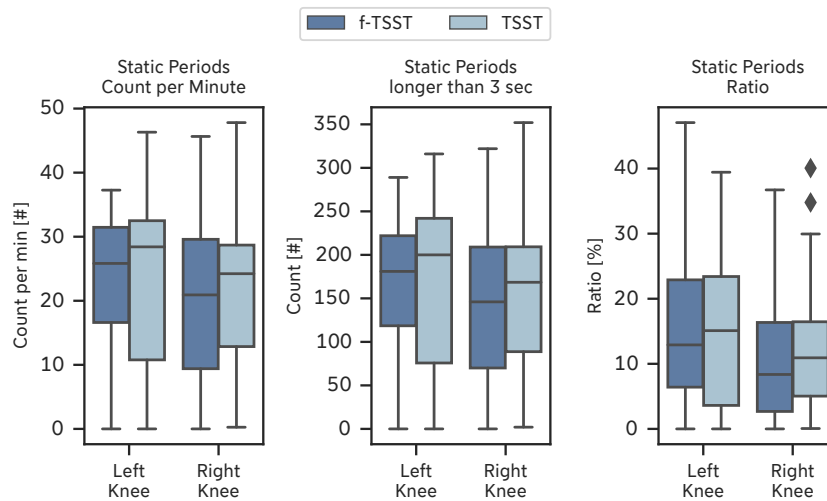
Figure 4.10: Expert features for the knees; (f-)TSST sitting.

In conclusion, based on the lack of statistical significance and the sometimes ambiguous or marginal differences, which could also be due to inaccurate pose estimation, the stressed condition could not be distinguished from the control condition in a seated position. This is at least the case for the techniques and features used in this thesis.

4.2.3 Gender differences

Since the stressed condition could only be differentiated from the control condition in a standing position, the investigation of gender differences was limited to this variation of the (f-)TSST. For
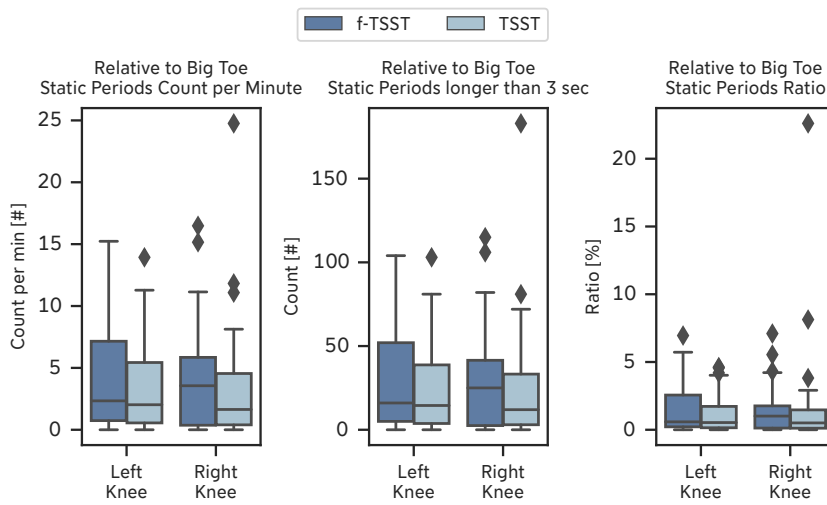
Figure 4.11: Expert features for the knees relative to corresponding big toe; (f-)TSST sitting.

this purpose, a statistical analysis was carried out, which, in addition to the procedure described in 3.4.1, also factored in the gender of the participant as a "between" variable. This resulted in some statistically significant features, which can be seen in Table 4.2. The statistical results of these features are displayed in Table B.8. As expected, both genders showed a stress reaction throughout the TSST based on the, in some cases drastic, increase in features related to static periods.

Table 4.2: Statistically significant gender differences regarding static periods (SP) for the mid hip, [1]relative to the neck; mean $\pm$ SD.

Metric	Female		Male	
	TSST	f-TSST	TSST	f-TSST
Max. Duration (s)	107.78 ± 44.79	90.04 ± 49.24	208.25 ± 93.62	136.50 ± 208.25
Mean Duration (s)	21.13 ± 3.59	20.09 ± 3.38	27.94 ± 6.47	23.15 ± 3.07
Ratio (%)	13.41 ± 7.07	11.65 ± 6.81	23.82 ± 8.38	19.37 ± 6.49
SD Duration (s)	12.86 ± 4.73	11.05 ± 4.69	22.76 ± 9.05	15.36 ± 5.12
Counts per Min[1]	29.91 ± 13.49	25.22 ± 11.66	44.96 ± 12.02	41.16 ± 11.80
Longer 3 Sec[1]	215.87 ± 97.18	182.87 ± 83.40	323 ± 86.07	291.05 ± 85.51
Ratio (%)[1]	10.26 ± 5.89	8.03 ± 4.72	17.91 ± 6.58	14.69 ± 5.26

Interestingly, the features concerned exclusively the mid hip keypoint, partly relative to the neck. Looking at the maximum duration of the static periods in seconds, for example, this increased, on average, by 53% for men, whereas there was only a 20% increase for women. The SD of the duration of static periods was also striking. There was a mean increase of 48% for male participants in the TSST, while for female participants it was only 16% more than in the f-TSST. The women

therefore tended to move more in the hip area during both conditions and the acute stress reaction
had a less dramatic effect on this region of their bodies. However, a clear reason explaining these
differences could not be found either through further analysis or in other studies.

4.2.4   Phases of (f-)TSST

For the analysis of the differences within the individual phases of the (f-)TSST, only the standing
variant of the (f-)TSST was considered. Additionally, none of the participants recorded with the
Kinect were included, due to the reasons explained in 3.1.4. Based on previous findings that static
periods are particularly meaningful for the stress level of the participants, the focus was on the
features that would characterize a freezing behavior. Figure 4.12 shows how the velocity of various
body parts changed during the individual phases.
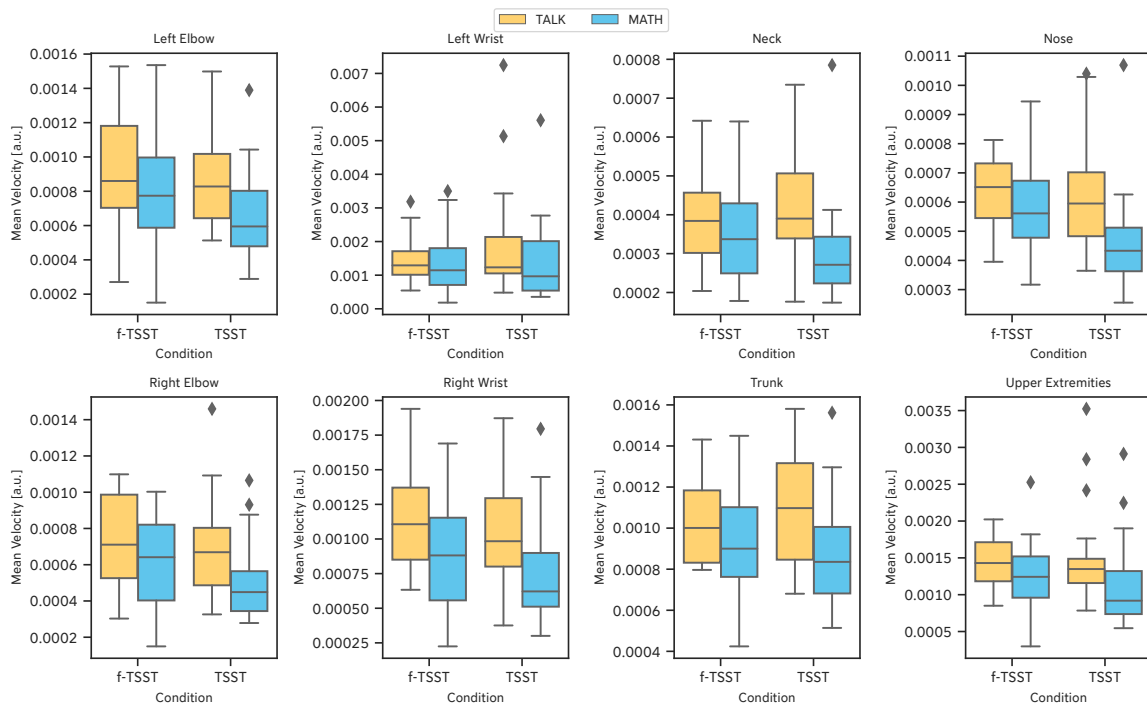
Figure 4.12: Generic features for different body parts during individual (f-)TSST phases.

It can be seen that there was a decrease in movement for most body parts throughout the TSST,
indicating an increased stress level. What could be observed, except for the left wrist, was that the
participants moved less during the math part of the (f-)TSST. This was true for both the TSST and
the control condition. Such a behavior suggests that the math part caused more acute stress than
the talk part. Looking at the head region, which was the most informative body part to distinguish

between the two conditions, there was a considerable difference between the two phases in the TSST. The observation is supported by the expert features in Figure 4.13.
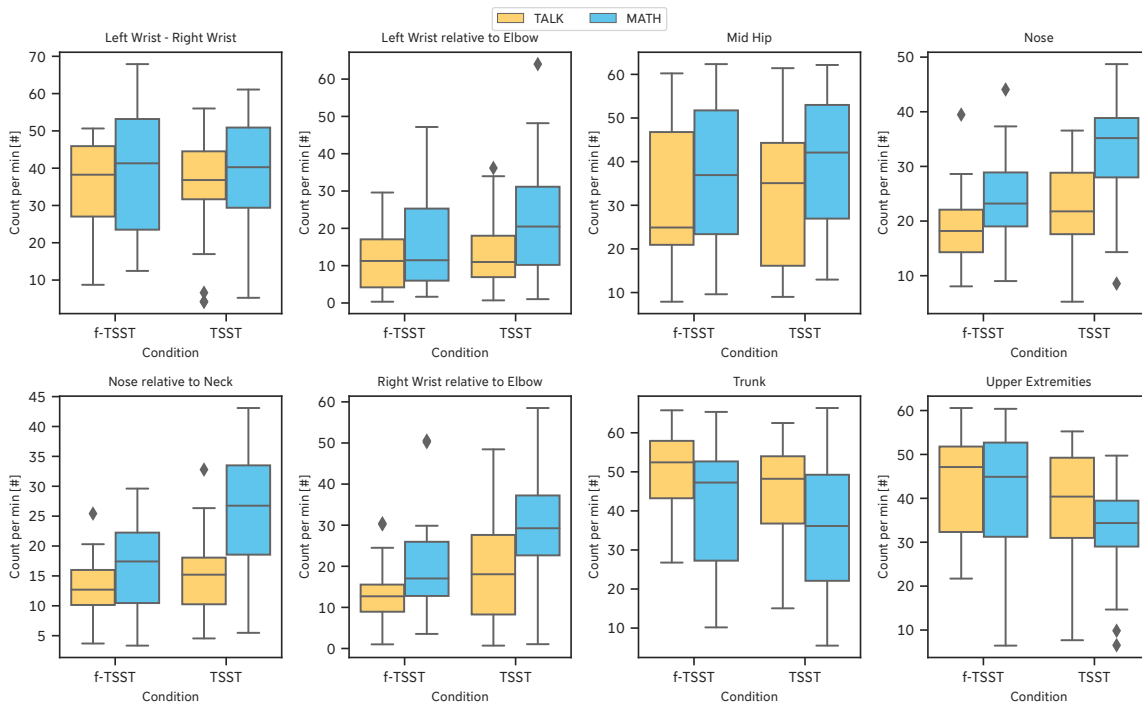
Figure 4.13: Expert features (SP) for different body parts during individual (f-)TSST phases.

Identified was, in most cases, an increase in static periods during the TSST and an additional increase during the math phase. The head region was again particularly indicative, and a substantial difference could be observed between the conditions, as well as the two phases.

In conclusion, the results showed a noticeable decrease in movement throughout the arithmetic task, indicating a greater stress response. This would further agree with the results of Abel, who came to a similar conclusion using IMU data [Abe22].

4.2.5 Camera Modality

As already mentioned in 3.1.3, about halfway through the study, there was a switch from a Microsoft Kinect camera to a Google Pixel 7A cell phone as the device for recording full-body videos. To investigate whether the used camera influenced motion-based stress detection, a statistical analysis was carried out for the (f-)TSST variant in a standing position. The procedure was analogous to 3.4.1 with the addition that the used camera was factored in as a between variable. The statistically significant features can be taken from Table 4.3.

Table 4.3: Statistically significant features regarding the different cameras.

Body Part	Channel	Metric	U	p	Hedges' g
Left & Right Ankle	vel_norm_rel2neck	SP Counts per min	402	0.034*	-1.312
Left Elbow	pos_norm_rel2neck	Entropy	52	0.014*	1.642
Left Elbow	vel_norm	Abs. Energy	448	<0.001***	-2.555
Neck	vel_norm	Mean Crossings	63	0.047*	1.443
Nose	vel_norm	Abs. Energy	431	0.001**	-2.5
Nose	vel_norm	Mean Crossings	50	0.011*	1.533
Nose	vel_norm_rel2neck	Mean Crossings	49	0.010*	1.765
Right Elbow	pos_norm_rel2neck	Entropy	43	0.005**	1.667
Right Elbow	vel_norm	Abs. Energy	452	<0.001***	-2.815
Right Wrist	vel	SD	42	0.005**	1.754
Trunk	pos_norm_rel2neck	Entropy	62	0.042*	1.449
Trunk	pos_norm_rel2neck	SD	60	0.034*	1.543
Trunk	vel_norm	Abs. Energy	459	<0.001***	-3.427
Trunk	vel_norm_rel2neck	Abs. Energy	37	0.003**	1.666
Trunk	vel_norm_rel2neck	SD	57	0.025*	1.286
Upper Extremities	pos_norm	Entropy	62	0.042*	1.454
Upper Extremities	pos_norm_rel2neck	Entropy	56	0.022*	1.680

Initially excluding the trunk and upper extremities as grouped body regions, it is noticeable that the remaining body parts showing significant differences were primarily the extremities, or body parts generally closer to a border of the frame. It is important to mention that the Kinect was used to record horizontally and the cell phone in vertical format. For the cell phone videos, this caused the keypoints showing significant differences, to be very close to the borders of the camera frame. Since the study environment did not change, the differences must be due to technical specifications. The biggest and probably most important differences are in the camera lenses. The Google Pixel 7A has a wide-angle camera with a field of view (FOV) of 80° and an ultra wide-angle camera with a FOV of 120°[1]. The Kinect, on the other hand, works in horizontal color mode with a FOV of 90°[2]. Wide-angle cameras lead to object distortion, making it more difficult to estimate its

---

[1]https://store.google.com/product/pixel_7a_specs?hl=de (visited on 02/27/2024)
[2]https://learn.microsoft.com/en-us/azure/kinect-dk/hardware-specification (visited on 02/29/2024)

distance, area, or direction [Fan21]. A subsequent pose estimation that should be as accurate as possible can be more difficult, which is why special techniques for pose estimation of distorted images are being actively developed [Mik20; Miu20]. This could have led to certain movements being over- or underestimated due to distortion. Additionally, even if the spatial conditions have not changed over the entire period of data collection, the lighting conditions were likely picked up differently by the two cameras. Lighting conditions can can have an influence on pose estimation [Ye22]. In table B.6, the evaluation (mean $\pm$ SD) for the Kinect camera and in table B.7 for the cell phone is shown. It can be seen that features that indicate more movement were often higher for the cell phone camera. However, this was not apparent for all features of this type. What limits the direct comparability is that these were two completely different groups of participants.

4.2.6 Classification

Since the statistical analysis only allowed a distinction to be made for the standing (f-)TSST variant, only these participants were considered for the ML-based classification. The best-performing pipeline achieved a mean accuracy of $68.5\% \pm 9.7\%$ and had the following configuration:

- Scaling: MinMaxScaler

- Feature Selection: RFE

- Classification: DecisionTree

The respective confusion matrix is shown in Figure 4.14. Table 4.4 provides an overview of the results for the different pipelines according to 3.4.2.
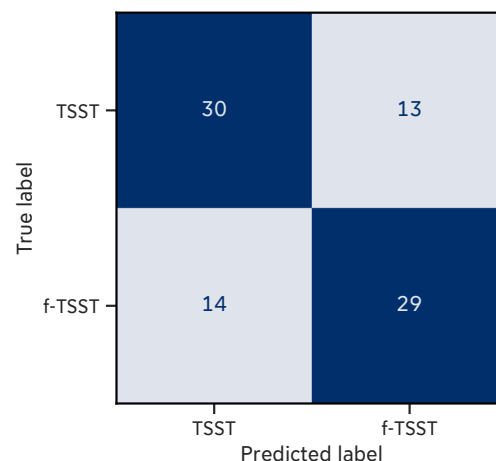
Figure 4.14: Confusion matrix for condition classification.

An evaluation based on the condition order did not provide any major differences in the average classification accuracy. The respective confusion matrices are displayed in Figure 4.15. The mean test accuracy for TSST-first was 65.2% and for f-TSST-first 72.5%, although the data sets were not equal in size and included different participants.

Table 4.4: Comparison of different ML pipelines; accuracy ± SD; best performing pipeline per classifier highlighted.

Feature selection	RFE		SelectKBest	
Scaling	MinMax	Standard	MinMax	Standard
Classification				
KNeighborsClassifier	60.4 ± 6.5	**60.7 ± 6.0**	55.7 ± 6.1	55.7 ± 5.0
SVC	56.0 ± 5.3	56.0 ± 8.5	**58.3 ± 13.1**	57.2 ± 12.1
DecisionTreeClassifier	**68.5 ± 9.7**	64.3 ± 7.7	57.9 ± 5.6	61.4 ± 6.8
AdaBoost	**63.7 ± 8.1**	59.7 ± 14.1	59.3 ± 11.5	57.9 ± 10.3
RandomForestClassifier	60.1 ± 12.3	**65.3 ± 4.9**	53.1 ± 11.7	55.6 ± 11.7
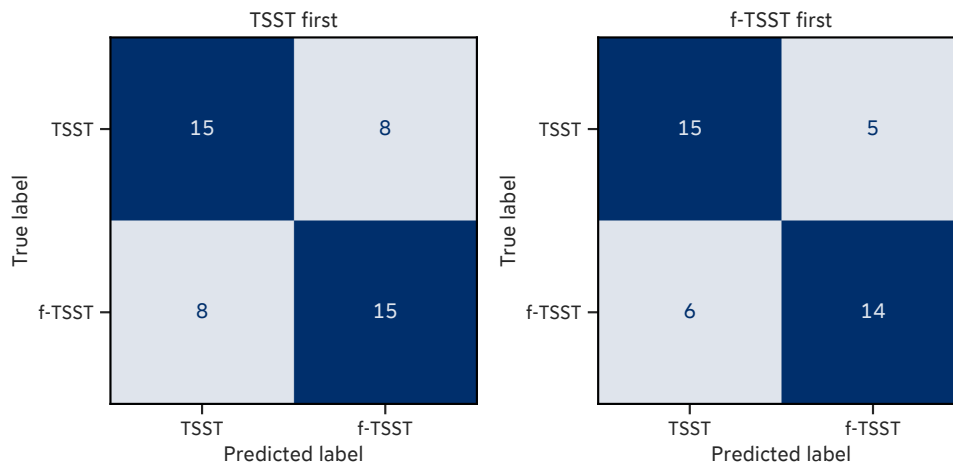
Figure 4.15: Confusion matrices for condition classification separated by condition order.

Comparing these results with studies by Richer et al. [Ric24] and Abel [Abe22], who achieved a mean test accuracy of 71.6% and 74.3% respectively, the results of this thesis are only slightly worse. It should be considered that in the two studies mentioned, the motion features were calculated on considerably more labor-intensive IMU data, making the results of this work quite promising.

In contrast to Abel [Abe22], there were smaller differences in classification accuracy by condition order. Thereby, 81.6% for TSST-first and 67.5% for f-TSST-first were achieved with a

comparable size of participants. This would suggest that the acute psychosocial stress responses on body posture and movements were only marginally influenced by the condition order. These findings would also be consistent with the statistical analysis regarding the effect of condition order in 4.2.1.

4.2.7 General Discussion & Limitations

In summary, the stressed condition could be distinguished from the control condition, at least when standing, using body posture and movement. The statistical analyses performed and a ML-based classification between the TSST and the f-TSST led to results that are comparable with similar studies [Abe22; Ric24]. Hence, this work supports the notion that bodily freezing behavior can be used as a significant characteristic for an acute psychosocial stress reaction. Notable is the used baseline, composed of the f-TSST [Wie13] and the placebo-TSST [Het09]. Even though the evaluated cortisol features clearly showed that there was no activation of the HPA-axis with the modified f-TSST, studies comprehensively investigating this protocol are still lacking. Even though this variant has been proven useful in comparable studies due to its better comparability to the TSST, it is still not optimal. As reported, the math part of the f-TSST still resulted in a stress response, which is probably because mental arithmetic, especially in front of other people, was not one of the strengths of many participants, even though the task was much easier compared to the TSST. Other participants, however, might have perceived this part as rather tiresome, especially considering the duration of 5 minutes. Nevertheless, it should be worthwhile to continue researching and to develop a baseline protocol that does not trigger a stress reaction in the participant, but which is directly comparable to the TSST.

Further, the change in gender composition of the panel in the second half of the study was also not optimal. Research suggests that for both men and women, interactions with the opposite gender result in increased discomfort and anxiety [McC91; Cho08]. Regarding the TSST, males and females showed greater cortisol increase when exposed to a panel including the opposite sex [Duc12]. Additionally, a meta-analysis revealed one of the lowest effect sizes concerning cortisol stress response for an all-female panel [Goo17], although no comparison to an all-male panel was made. Even though the effect was not investigated in this thesis, it would be advisable for future studies to follow the original protocol and have both genders represented on the panel.

The same applies to the used camera. As it was established that there was a, in some cases significant, difference in the features between the cameras. Therefore, the same camera should be used for the entire study. This makes the results more comparable and does not introduce any additional variables into the analyses.

Furthermore, the results are limited by the data used and its processing. The selection of candidates was based on a digital screening to check prerequisites for participation in the study. However, the actual participants were, except for physical measurements, not examined, and it can therefore not be ruled out that there were participants who should not have been allowed to take part in the study. Additionally, only young people participated in the study. Future studies should involve different age groups and potentially review the eligibility criteria more rigorously. In addition, a study with even more participants would be recommended to achieve a better generalizability of the results. Nevertheless, the data set for this thesis was already relatively extensive, with a total of 83 participants, whose data were complete and could therefore be included in the analysis.

For the seated participants, normalization was only performed for the upper body, as the sitting positions greatly varied during the (f-)TSST. This may have had an influence on how successful differences between the conditions were able to be observed. To solve this problem, a baseline could be recorded beforehand, in which the participant sits upright with both feet firmly on the ground to take measurements for later normalization.

The identification of the start and end of the (f-)TSST using a clapperboard was also not optimal. This had to be done because no system time was stored in the metadata for the videos, and therefore no synchronization with the times tracked by the panel for the start and end of the (f-)TSST was possible. It cannot be excluded that it took different lengths of time to sit down or to start, which could be caused by a technical error appearing just before the intended start, causing a delay after the clapperboard was closed. Furthermore, the manual determination of start and end times is very time-consuming. Future studies could remedy this by using a lamp with a visible light within the video, that is assigned different meanings depending on its color. The times within a video could thus be extracted automatically, based on the light filling out the video frame.

Another limiting factor was OpenPose itself and its data processing. In some cases, there were non-reproducible errors in OpenPose or an output that proved to be unusable only after extensively checking the data manually. This involved unpredictable shifts of the output in the 2D plane, sometimes minutes of missing pose estimation, or considerable time lags. Filling in missing frames using linear interpolation could also be inappropriate, as whole-body motion is inherently redundant and nonlinear [Fur17]. Furthermore, a standardized way of calculating thresholds, crucial for features like self-touching, which have been proven to be informative in other studies, should be developed. A future comparison with other pose estimation frameworks, interpolation techniques, and optimized features would be a useful extension.

A substantial drawback of the data collection was that different stress effects were examined in the course of the study. During the (f-)TSST, a total of seven electrodes were attached to the skin of each participant, which were connected to different instruments. This might have negatively influenced the baseline movement and the changes in movement due to an acute stress reaction. The participants may have actively tried to move less so that no cable was pulled out of a measurement instrument, or the cable pulled on the electrodes when they were under tension and thus pulled uncomfortably on the skin or lost contact. If possible, future studies should avoid wiring the participants to avoid any inherent restriction of movement.

Chapter 5

Conclusion & Outlook

This bachelor thesis presented a comprehensive analysis of bodily movement changes as an acute psychosocial stress response. Using camera videos of the whole body and OpenPose as the pose estimation framework, a contactless distinction between the stressed condition and the baseline for standing participants was achieved. For this purpose, different statistical metrics and features characterizing certain behaviors based on literature or observations during data acquisition were calculated and analyzed using statistics and ML. The TSST as the gold standard has proven to be a reliable tool to induce stress in participants in a laboratory setting. Despite the mentioned limitations, the f-TSST variant used proved to be a functional baseline with good comparability to the TSST. This was confirmed by the calculated endocrinological measures, which all showed a significant difference between the conditions regardless of condition order and whether the participants performed the (f-)TSST while standing or sitting.

For the successful distinction between the conditions in the standing variant, the head turned out to be the most meaningful body part. During the TSST, its movement, also relative to the neck, decreased significantly. This was confirmed by other features quantifying SP. The stress response was shown by a significant decrease in movement in this body region, indicating a freezing behavior and a more tense posture, which was also found in previous studies. Features such as self-touching, body-sway, or non-smooth movement did not prove to be significant in this study.

It was not possible to achieve a differentiation between the conditions while sitting with the features calculated in this thesis. Even though the head, as the significant body region in the standing variant, showed a reduction in movement in the seated variation as well, the differences were minimal. The leg bouncing feature, which only applied to the seated participants, showed that there was an increased knee bouncing during the TSST, but the results were not significant.

To the best of my knowledge, this is the first work to examine a seated variant, and therefore no comparison can be made with other findings.

In contrast to other studies, there was a difference between the genders, but this was limited to hip movements. Men and women both showed a decrease in movement in the TSST, but the effect was smaller for women, who tended to move more in this body region throughout both conditions. However, no robust explanation for this behavior was found through literature or further analysis.

A comparison of the math and talk phase of the standing variant showed a greater stress reaction during the math part. This was characterized by a freezing behavior in different parts of the body. A comparable study showed similar findings.

During the data collection, there was a switch from a Microsoft Kinect to a Google Pixel 7A for video recording. The effect of the switch revealed some significant findings. Mainly affected were physical extremities or body parts that were closer to the edge of the frame and could have led to differences due to distortion. Therefore, as in other studies, one camera should be chosen and remain the same throughout the data acquisition.

A ML-based classification between the TSST and the f-TSST with a mean accuracy of 68.5% is not far from comparable results, which were based on a considerably more sophisticated data collection technique using IMU data.

In conclusion, despite the limitations, the results of this work are promising and provide a basis for further research. Bodily freezing has been confirmed as a characteristic for an acute psychosocial stress response triggered by the TSST. Both statistical analysis and ML-based classification have led to confident results that automated stress detection using contactless motion analysis is possible. However, these results also show that there is still a long way to go for reliable detection, preferably outside of a laboratory.

Future studies should optimize the data collection process by not wiring participants and always using the same camera to prevent potentially causing movement restrictions and improve comparability between participants. Further optimizations regarding the feature calculation would also be advisable. In particular, the thresholds should be adjusted and additional features added. Overall, an attempt could be made to use a more natural stress protocol and move away from a standardized laboratory environment. A long-term goal would be a truly comprehensive understanding of stress and how it manifests itself through easily measurable markers in the body, which cannot only be determined in the laboratory. This would make it possible to recognize repeated stress at an early stage and take countermeasures to prevent it from becoming chronic. Research into psycho-motoric models could create the basis for characterizing humans' inner states during an acute, psychosocial stress reaction from purely contactless measurements.

Appendix A

Additional Figures
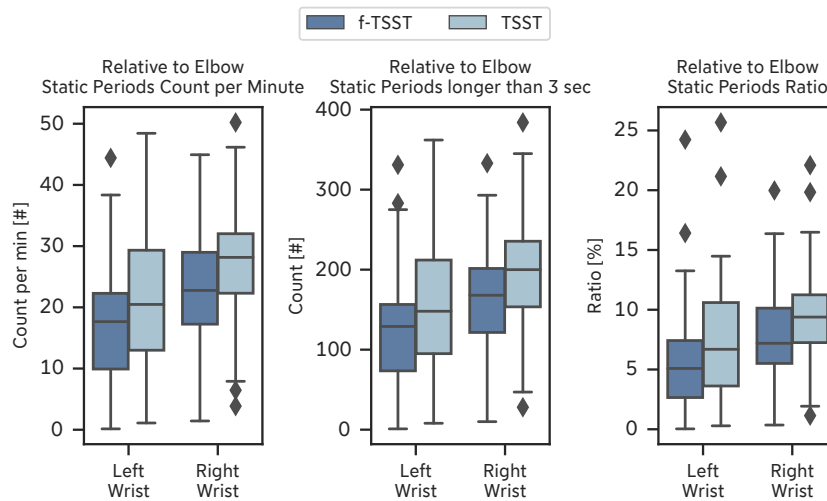
Figure A.1: Static periods for the wrists relative to corresponding elbow; (f-)TSST standing.
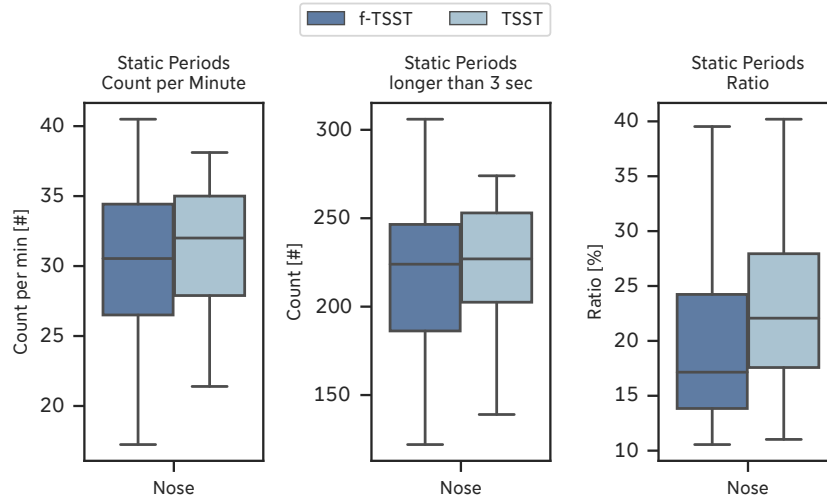
Figure A.2: Expert features for the nose; (f-)TSST sitting.
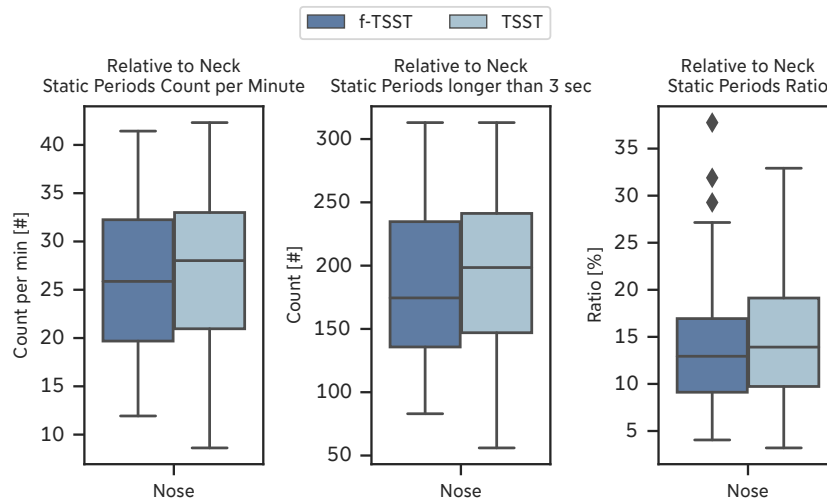
Figure A.3: Expert features for the nose relative to the neck; (f-)TSST sitting.

Appendix B

Additional Tables

Table B.1: Metrics for the expert features.

Metric	Definition
count_per_min	Number of occurences per min
max_duration_sec	Longest duration in s
mean_duration_sec	Mean duration in s
longer_than_3sec	Number of intervals longer than 3 s
std_duration_sec	SD of duration in s
ratio_percent	Ratio of total time in %
frames_below_threshold	Number of frames below threshold

Table B.2: Thresholds and body parts for velocity norm.

Body Part	Threshold
Nose	5×10^{-8}
Mid Hip	2.5×10^{-7}
Trunk	5×10^{-7}
{L/R} Wrist	5×10^{-7}
Upper Extremities	1×10^{-6}

Table B.3: Thresholds and body parts for velocity norm relative to the neck.

Body Part	Threshold
Nose	1×10^{-7}
{L/R} Ankle	5×10^{-7}
Mid Hip	2.5×10^{-7}
Trunk	1×10^{-6}
{L/R} Wrist	5×10^{-7}
Upper Extremities	2.5×10^{-6}

Table B.4: Statistical results of all generic features.

Body Part	Channel	Metric	W	p	Hedges' g
Left Elbow	pos_norm	SD	398	>0.999	0.188
		Entropy	469	>0.999	0.081
	pos_norm_rel2neck	FFT Centroid	435	>0.999	-0.004
		FFT Skewness	434	>0.999	0.085
		SD	378	>0.999	0.129
		Entropy	427	>0.999	0.056
		FFT Kurtosis	459	>0.999	0.066
		FFT Variance	420	>0.999	0.078
	vel	SD	436	>0.999	-0.069
	vel_norm	Abs. Energy	458	>0.999	-0.018
		Mean	344	>0.999	-0.226
		Mean Crossings	303	>0.999	-0.273
	vel_norm_rel2neck	Abs. Energy	430	>0.999	0.008
		Mean	339	>0.999	-0.226
		SD	473	>0.999	0.063
		Mean Crossings	317	>0.999	-0.275
	vel_norm_rel2neck_2d	FFT Centroid	468	>0.999	-0.021
		FFT Skewness	408	>0.999	-0.052
		FFT Kurtosis	444	>0.999	-0.050
		FFT Variance	447	>0.999	-0.034
Left Wrist	pos_norm	SD	333	>0.999	0.222
		Entropy	456	>0.999	0.285
	pos_norm_rel2leftelbow	FFT Centroid	443	>0.999	0.095
		FFT Skewness	381	>0.999	0.124
		SD	312	>0.999	0.350
		Entropy	449	>0.999	0.065
		FFT Kurtosis	435	>0.999	0.035
		FFT Variance	400	>0.999	0.143
	pos_norm_rel2neck	FFT Centroid	385	>0.999	0.234

		FFT Skewness	459	>0.999	-0.044
		SD	353	>0.999	0.180
		Entropy	463	>0.999	0.272
		FFT Kurtosis	439	>0.999	-0.095
		FFT Variance	339	>0.999	0.281
	vel	SD	350	>0.999	0.003
	vel_norm	Abs. Energy	385	>0.999	0.151
		Mean	368	>0.999	-0.079
		Mean Crossings	443.500	>0.999	-0.046
	vel_norm_rel2leftelbow	Abs. Energy	456	>0.999	0.152
		Mean	383	>0.999	-0.061
		SD	417	>0.999	-0.035
		Mean Crossings	448	>0.999	0.020
	vel_norm_rel2leftelbow_2d	FFT Centroid	426	>0.999	0.133
		FFT Skewness	456	>0.999	-0.011
		Zero Crossings	209	>0.999	-0.239
		FFT Kurtosis	417	>0.999	0.097
		FFT Variance	454	>0.999	0.077
	vel_norm_rel2neck	Abs. Energy	400	>0.999	0.145
		Mean	361	>0.999	-0.083
		SD	368	>0.999	-0.056
		Mean Crossings	453	>0.999	-0.018
	vel_norm_rel2neck_2d	FFT Centroid	438	>0.999	0.144
		FFT Skewness	429	>0.999	-0.067
		Zero Crossings	214	>0.999	-0.239
		FFT Kurtosis	384	>0.999	0.188
		FFT Variance	470	>0.999	0.085
Neck	pos_norm	SD	253	>0.999	0.350
	vel	SD	464	>0.999	-0.025
	vel_norm	Mean	376	>0.999	-0.138
		Mean Crossings	294	>0.999	-0.280
Nose	pos_norm	SD	290	>0.999	0.295
		Entropy	412	>0.999	-0.043

	pos_norm_rel2neck	FFT Centroid	307	>0.999	-0.216
		FFT Skewness	366	>0.999	0.144
		SD	364	>0.999	0.135
		Entropy	329	>0.999	-0.168
		FFT Kurtosis	386	>0.999	0.123
		FFT Variance	387	>0.999	-0.158
	vel	SD	366	>0.999	-0.315
	vel_norm	Abs. Energy	320	>0.999	-0.225
		Mean	140	0.006**	-0.537
		Mean Crossings	217	0.400	-0.435
	vel_norm_rel2neck	Abs. Energy	241	>0.999	-0.273
		Mean	156	0.015*	-0.501
		SD	268	>0.999	-0.253
		Mean Crossings	227	0.628	-0.380
	vel_norm_rel2neck_2d	FFT Centroid	392	>0.999	0.055
		FFT Skewness	269	>0.999	-0.389
		FFT Kurtosis	378	>0.999	-0.143
		FFT Variance	379	>0.999	0.097
Right Elbow	pos_norm	SD	266	>0.999	0.293
		Entropy	430	>0.999	0.160
	pos_norm_rel2neck	FFT Centroid	385	>0.999	-0.188
		FFT Skewness	293	>0.999	0.380
		SD	286	>0.999	0.230
		Entropy	363	>0.999	-0.038
		FFT Kurtosis	300	>0.999	0.353
		FFT Variance	423	>0.999	-0.061
	vel	SD	388	>0.999	-0.204
	vel_norm	Abs. Energy	377	>0.999	-0.116
		Mean	374	>0.999	-0.196
		Mean Crossings	356	>0.999	-0.263
	vel_norm_rel2neck	Abs. Energy	378	>0.999	-0.010
		Mean	340	>0.999	-0.254
		SD	397	>0.999	0.016

		Mean Crossings	362	>0.999	-0.227
	vel_norm_rel2neck_2d	FFT Centroid	443	>0.999	-0.005
		FFT Skewness	434	>0.999	-0.069
		FFT Kurtosis	427	>0.999	-0.039
		FFT Variance	458	>0.999	0.021
Right Wrist	pos_norm	SD	276	>0.999	0.388
		Entropy	366	>0.999	-0.058
	pos_norm_rel2neck	FFT Centroid	457	>0.999	0.010
		FFT Skewness	359	>0.999	0.223
		SD	318	>0.999	0.341
		Entropy	382	>0.999	-0.109
		FFT Kurtosis	387	>0.999	0.202
		FFT Variance	430	>0.999	0.092
	pos_norm_rel2rightelbow	FFT Centroid	369	>0.999	-0.168
		FFT Skewness	374	>0.999	0.212
		SD	393	>0.999	0.338
		Entropy	332	>0.999	-0.146
		FFT Kurtosis	379	>0.999	0.184
		FFT Variance	412	>0.999	-0.070
	vel	SD	327	>0.999	-0.140
	vel_norm	Abs. Energy	455	>0.999	-0.018
		Mean	359	>0.999	-0.181
		Mean Crossings	319	>0.999	-0.270
	vel_norm_rel2neck	Abs. Energy	414	>0.999	0.002
		Mean	348	>0.999	-0.198
		SD	415	>0.999	-0.028
		Mean Crossings	316	>0.999	-0.274
	vel_norm_rel2neck_2d	FFT Centroid	469	>0.999	0.007
		FFT Skewness	471	>0.999	-0.003
		FFT Kurtosis	458	>0.999	-0.017
		FFT Variance	461	>0.999	0.024
	vel_norm_rel2rightelbow	Abs. Energy	416	>0.999	-0.020
		Mean	335	>0.999	-0.165

		SD	425	>0.999	-0.046
		Mean Crossings	329	>0.999	-0.189
	vel_norm_rel2rightelbow_2d	FFT Centroid	457	>0.999	-0.003
		FFT Skewness	466	>0.999	0.010
		FFT Kurtosis	430	>0.999	0.045
		FFT Variance	462	>0.999	-0.032
Trunk	pos_norm	SD	269	>0.999	0.259
		Entropy	467	>0.999	0.067
	pos_norm_rel2neck	FFT Centroid	443	>0.999	-0.125
		FFT Skewness	335	>0.999	0.247
		SD	269	>0.999	0.514
		Entropy	422	>0.999	0.032
		FFT Kurtosis	345	>0.999	0.251
		FFT Variance	460	>0.999	-0.039
	vel	SD	443	>0.999	-0.108
	vel_norm	Abs. Energy	433	>0.999	-0.033
		Mean	389	>0.999	-0.133
	vel_norm_rel2neck	Abs. Energy	414	>0.999	0.075
		Mean	368	>0.999	-0.167
		SD	447	>0.999	0.147
	vel_norm_rel2neck_2d	FFT Centroid	457	>0.999	-0.000
		FFT Skewness	370	>0.999	-0.239
		FFT Kurtosis	450	>0.999	-0.057
		FFT Variance	473	>0.999	0.008
Upper Extremities	pos_norm	SD	337	>0.999	0.226
		Entropy	452	>0.999	0.152
	pos_norm_rel2neck	FFT Centroid	458	>0.999	-0.005
		FFT Skewness	328	>0.999	0.229
		SD	304	>0.999	0.309
		Entropy	443	>0.999	0.087
		FFT Kurtosis	358	>0.999	0.223
		FFT Variance	409	>0.999	0.077
	vel	SD	405	>0.999	-0.063

vel_norm	Abs. Energy	399	>0.999	0.113
	Mean	328	>0.999	-0.141
vel_norm_rel2neck	Abs. Energy	380	>0.999	0.136
	Mean	318	>0.999	-0.162
	SD	380	>0.999	0.036
vel_norm_rel2neck_2d	FFT Centroid	462	>0.999	0.050
	FFT Skewness	408	>0.999	-0.083
	FFT Kurtosis	440	>0.999	-0.015
	FFT Variance	447	>0.999	0.034

Table B.5: Statistical results of all expert features.

Body part	Channel	Metric	W	p	Hedges' g
Left & Right Ankle	Static Periods	Counts per Minute	345	>0.999	-0.129
		Max. Duration (s)	424	>0.999	0.094
		Mean Duration (s)	320	>0.999	0.252
		Ratio (%)	330	>0.999	0.197
		SD Duration (s)	382	>0.999	0.177
		Longer than 3 Seconds	361	>0.999	-0.129
Left Wrist	vel_norm_rel2leftelbow	Counts per Minute	284	>0.999	0.351
		Max. Duration (s)	275	>0.999	0.103
		Mean Duration (s)	236	0.924	0.297
		Ratio (%)	281	>0.999	0.324
		SD Duration (s)	289	>0.999	0.156
		Longer than 3 Seconds	268.500	>0.999	0.363
Left Wrist & Nose	euclidean_distance	Mean	382	>0.999	-0.135
		SD	327	>0.999	0.200
		Frames below threshold	117.500	>0.999	-0.187
Left Wrist & Right Wrist	euclidean_distance	Mean	293	>0.999	-0.309
		SD	371	>0.999	0.240
		Frames below threshold	218	>0.999	0.191
	vel_norm	Counts per Minute	458	>0.999	-0.030
		Max. Duration (s)	304	>0.999	0.440
		Mean Duration (s)	283	>0.999	0.450
		Ratio (%)	298	>0.999	0.316
		SD Duration (s)	288	>0.999	0.460
		Longer than 3 Seconds	454	>0.999	-0.022
	vel_norm_rel2neck	Counts per Minute	373	>0.999	0.121
		Max. Duration (s)	313	>0.999	0.374
		Mean Duration (s)	283	>0.999	0.454
		Ratio (%)	280	>0.999	0.362
		SD Duration (s)	294	>0.999	0.487

		Longer than 3 Seconds	329.500	>0.999	0.139
Mid Hip	vel_norm	Counts per Minute	432	>0.999	0.145
		Max. Duration (s)	239.500	>0.999	0.558
		Mean Duration (s)	246	>0.999	0.552
		Ratio (%)	307	>0.999	0.352
		SD Duration (s)	243	>0.999	0.612
		Longer than 3 Seconds	419.500	>0.999	0.163
	vel_norm_rel2neck	Counts per Minute	323	>0.999	0.293
		Max. Duration (s)	251	>0.999	0.430
		Mean Duration (s)	225	0.575	0.543
		Ratio (%)	279	>0.999	0.402
		SD Duration (s)	250	>0.999	0.491
		Longer than 3 Seconds	329.500	>0.999	0.313
Nose	vel_norm	Counts per Minute	112	<0.001***	0.666
		Max. Duration (s)	399	>0.999	-0.059
		Mean Duration (s)	216	0.382	0.494
		Ratio (%)	72	<0.001***	0.707
		SD Duration (s)	347	>0.999	0.162
		Longer than 3 Seconds	129.500	0.003**	0.684
	vel_norm_rel2neck	Counts per Minute	107	<0.001***	0.680
		Max. Duration (s)	323	>0.999	0.082
		Mean Duration (s)	325	>0.999	0.265
		Ratio (%)	122	0.002**	0.609
		SD Duration (s)	347	>0.999	0.132
		Longer than 3 Seconds	121	0.001**	0.702
Right Wrist	vel_norm_rel2rightelbow	Counts per Minute	271	>0.999	0.406
		Max. Duration (s)	361	>0.999	0.019
		Mean Duration (s)	312	>0.999	0.298
		Ratio (%)	290	>0.999	0.393
		SD Duration (s)	358	>0.999	0.065
		Longer than 3 Seconds	272.500	>0.999	0.426
Right Wrist & Nose	euclidean_distance	Mean	308	>0.999	-0.241
		SD	289	>0.999	0.339

		Frames below threshold	109	>0.999	0.077
Trunk	vel_norm	Counts per Minute	323	>0.999	-0.334
		Max. Duration (s)	285	>0.999	0.306
		Mean Duration (s)	319	>0.999	0.281
		Ratio (%)	433	>0.999	0.116
		SD Duration (s)	307	>0.999	0.272
		Longer than 3 Seconds	308	>0.999	-0.328
	vel_norm_rel2neck	Counts per Minute	255	>0.999	-0.442
		Max. Duration (s)	305	>0.999	0.348
		Mean Duration (s)	281	>0.999	0.342
		Ratio (%)	423	>0.999	0.111
		SD Duration (s)	253	>0.999	0.406
		Longer than 3 Seconds	254.500	>0.999	-0.432
Upper Extremities	vel_norm	Counts per Minute	283	>0.999	-0.475
		Max. Duration (s)	158	0.064	0.667
		Mean Duration (s)	230	0.715	0.546
		Ratio (%)	295	>0.999	0.288
		SD Duration (s)	191	0.112	0.576
		Longer than 3 Seconds	274.500	>0.999	-0.482
	vel_norm_rel2neck	Counts per Minute	302	>0.999	-0.314
		Max. Duration (s)	228	0.656	0.398
		Mean Duration (s)	301	>0.999	0.322
		Ratio (%)	372	>0.999	0.196
		SD Duration (s)	256	>0.999	0.361
		Longer than 3 Seconds	285.500	>0.999	-0.321

Table B.6: Statistically significant features for the kinect camera; mean $\pm$ SD.

Body Part	Channel	Metric	f-TSST	TSST
Left & Right Ankle	vel_norm_rel2neck	SP Counts per Minute	70.16 ± 12.29	67.64 ± 14.56
Left Elbow	pos_norm_rel2neck	Entropy	10.10 ± 0.09	10.11 ± 0.04
	vel_norm	Abs. Energy	0.20 ± 0.04	0.20 ± 0.04
Neck	vel_norm	Mean Crossings	3444.80 ± 640.54	3270.91 ± 621.64
Nose	vel_norm	Abs. Energy	0.16 ± 0.03	0.15 ± 0.03
		Mean Crossings	3708.41 ± 444.07	3594.55 ± 281.72
	vel_norm_rel2neck	Mean Crossings	4863.68 ± 777.59	4569.45 ± 600.37
Right Elbow	pos_norm_rel2neck	Entropy	10.11 ± 0.09	10.11 ± 0.03
	vel_norm	Abs. Energy	0.15 ± 0.03	0.15 ± 0.03
Right Wrist	vel	SD	1.82 ± 0.29	1.78 ± 0.27
Trunk	pos_norm_rel2neck	Entropy	10.11 ± 0.09	10.12 ± 0.03
	pos_norm_rel2neck	SD	0.00416 ± 0.00125	0.00436 ± 0.00119
	vel_norm	Abs. Energy	0.32627 ± 0.06268	0.32216 ± 0.05920
	vel_norm_rel2neck	Abs. Energy	0.04312 ± 0.01710	0.03881 ± 0.01129
	vel_norm_rel2neck	SD	0.00078 ± 0.00009	0.00077 ± 0.00008
Upper Extremities	pos_norm	Entropy	10.11 ± 0.09	10.13 ± 0.04
	pos_norm_rel2neck	Entropy	10.09 ± 0.09	10.11 ± 0.04

Table B.7: Statistically significant features for the phone; mean $\pm$ SD.

Body Part	Channel	Metric	f-TSST	TSST
Left & Right Ankle	vel_norm_rel2neck	SP Counts per Minute	51.50 ± 16.93	49.54 ± 15.01
Left Elbow	pos_norm_rel2neck	Entropy	10.17 ± 0.03	10.17 ± 0.02
	vel_norm	Abs. Energy	0.10 ± 0.07	0.10 ± 0.07
Neck	vel_norm	Mean Crossings	4186.50 ± 517.40	3977.81 ± 492.11
Nose	vel_norm	Abs. Energy	0.07 ± 0.09	0.05 ± 0.03
		Mean Crossings	4493.26 ± 500.48	4099.55 ± 600.10
	vel_norm_rel2neck	Mean Crossings	6253.43 ± 872.11	5754.43 ± 938.72
Right Elbow	pos_norm_rel2neck	Entropy	10.18 ± 0.03	10.17 ± 0.03
	vel_norm	Abs. Energy	0.07 ± 0.05	0.06 ± 0.04
Right Wrist	vel	SD	2.71 ± 0.78	2.54 ± 0.86
Trunk	pos_norm_rel2neck	Entropy	10.18 ± 0.03	10.17 ± 0.03
	pos_norm_rel2neck	SD	0.00502 ± 0.00078	0.00633 ± 0.00151
	vel_norm	Abs. Energy	0.12641 ± 0.09454	0.12186 ± 0.10021
	vel_norm_rel2neck	Abs. Energy	0.06454 ± 0.01760	0.07340 ± 0.04022
	vel_norm_rel2neck	SD	0.00090 ± 0.00016	0.00098 ± 0.00033
Upper Extremities	pos_norm	Entropy	10.17 ± 0.04	10.17 ± 0.03
	pos_norm_rel2neck	Entropy	10.17 ± 0.04	10.16 ± 0.03

Table B.8: Statistically significant features regarding gender differences for SP.

Body Part	Channel	Metric	U	p	Hedges' g
Mid Hip	vel_norm	Max. duration (s)	50	0.012*	1.698
		Mean duration (s)	52	0.015*	1.590
		Ratio (%)	59	0.033*	1.636
		SD (s)	47	0.009**	1.697
	vel_norm_rel2neck	Counts per Min	53	0.017*	1.590
		Longer 3 Sec	57	0.026*	1.580
		Ratio (%)	53	0.017*	1.604

List of Figures

List of Tables

Bibliography

[Abe19]   Luca Abel, Robert Richer, Arne Küderle, Stefan Gradl, Bjoern M. Eskofier, and
            Nicolas Rohleder. "Classification of Acute Stress-Induced Response Patterns".
            In: *Proceedings of the 13th EAI International Conference on Pervasive Com-
            puting Technologies for Healthcare*. PervasiveHealth'19. New York, NY, USA:
            Association for Computing Machinery, May 20, 2019, pp. 366–370. ISBN: 978-1-
            4503-6126-2. DOI: 10.1145/3329189.3329231. URL: https://dl.acm.org/doi/
            10.1145/3329189.3329231 (visited on 02/17/2024).

[Abe21]   Kenta Abe, Ken-Ichi Tabei, Keita Matsuura, Kazuyuki Kobayashi, and Tomoyuki
            Ohkubo. "OpenPose-based Gait Analysis System For Parkinson's Disease Pa-
            tients From Arm Swing Data". In: *2021 International Conference on Advanced
            Mechatronic Systems (ICAMechS)*. 2021 International Conference on Advanced
            Mechatronic Systems (ICAMechS). ISSN: 2325-0690. Dec. 2021, pp. 61–65. DOI:
            10.1109/ICAMechS54019.2021.9661562. URL: https://ieeexplore.ieee.org/
            document/9661562 (visited on 01/05/2024).

[Abe22]   Luca Abel. "Machine Learning-Based Detection of Acute Psychosocial Stress
            from Dynamic Movements". Master Thesis. Friedrich-Alexander-Universität
            Erlangen-Nürnberg, 2022. URL: https://www.mad.tf.fau.de/files/2022/
            06/MA_Abel_Luca.pdf (visited on 11/09/2023).

[Aig15]   Jonathan Aigrain, Séverine Dubuisson, Marcin Detyniecki, and Mohamed Chetouani.
            "Person-specific behavioural features for automatic stress detection". In: *2015 11th
            IEEE International Conference and Workshops on Automatic Face and Gesture
            Recognition (FG)*. 2015 11th IEEE International Conference and Workshops on
            Automatic Face and Gesture Recognition (FG). Vol. 03. May 2015, pp. 1–6. DOI:

10.1109/FG.2015.7284844. URL: https://ieeexplore.ieee.org/document/7284844 (visited on 12/11/2023).

[Aig18]   Jonathan Aigrain, Michel Spodenkiewicz, Séverine Dubuisson, Marcin Detyniecki, David Cohen, and Mohamed Chetouani. "Multimodal Stress Detection from Multiple Assessments". In: *IEEE Transactions on Affective Computing* 9.4 (Oct. 2018). Conference Name: IEEE Transactions on Affective Computing, pp. 491–506. ISSN: 1949-3045. DOI: 10.1109/TAFFC.2016.2631594. URL: https://ieeexplore.ieee.org/document/7752842 (visited on 12/19/2023).

[Ala11]   Kaat Alaerts, Evelien Nackaerts, Pieter Meyns, Stephan P. Swinnen, and Nicole Wenderoth. "Action and emotion recognition from point light displays: an investigation of gender differences". In: *PloS One* 6.6 (2011), e20989. ISSN: 1932-6203. DOI: 10.1371/journal.pone.0020989.

[All03]   R.P. Allen, D. Picchietti, W.A. Hening, C. Trenkwalder, A.S. Walters, and J. Montplaisi. "Restless legs syndrome: Diagnostic criteria, special considerations, and epidemiology. A report from the restless legs syndrome diagnosis and epidemiology workshop at the National Institutes of Health". In: *Sleep Medicine* 4.2 (2003), pp. 101–119. ISSN: 1389-9457. DOI: 10.1016/S1389-9457(03)00010-8.

[All14]   Andrew P. Allen, Paul J. Kennedy, John F. Cryan, Timothy G. Dinan, and Gerard Clarke. "Biological and psychological markers of stress in humans: Focus on the Trier Social Stress Test". In: *Neuroscience & Biobehavioral Reviews* 38 (Jan. 2014), pp. 94–124. ISSN: 01497634. DOI: 10.1016/j.neubiorev.2013.11.005. URL: https://linkinghub.elsevier.com/retrieve/pii/S0149763413002728 (visited on 04/29/2022).

[APA20]   APA. *Stress in America™ 2020: A National Mental Health Crisis.* American Psychological Association, 2020. URL: https://www.apa.org/news/press/releases/stress/2020/sia-mental-health-crisis.pdf.

[Arm14]   Richard A. Armstrong. "When to use the Bonferroni correction". In: *Ophthalmic and Physiological Optics* 34.5 (2014), pp. 502–508. ISSN: 1475-1313. DOI: 10.1111/opo.12131. URL: https://onlinelibrary.wiley.com/doi/10.1111/opo.12131 (visited on 02/22/2024).

[Atk04]   Anthony P Atkinson, Winand H Dittrich, Andrew J Gemmell, and Andrew W
            Young. "Emotion Perception from Dynamic and Static Body Expressions in Point-
            Light and Full-Light Displays". In: *Perception* 33.6 (June 1, 2004). Publisher:
            SAGE Publications Ltd STM, pp. 717–746. ISSN: 0301-0066. DOI: 10.1068/p5096.
            URL: https://doi.org/10.1068/p5096 (visited on 11/10/2023).

[Bal00]   Gene Ball and Jack Breese. "Relating Personality and Behavior: Posture and
            Gestures". In: *Affective Interactions: Towards a New Generation of Computer
            Interfaces*. Ed. by Ana Paiva. Lecture Notes in Computer Science. Berlin, Hei-
            delberg: Springer, 2000, pp. 196–203. ISBN: 978-3-540-44559-3. DOI: 10.1007/
            10720296_14. URL: https://doi.org/10.1007/10720296_14 (visited on
            01/03/2024).

[Bar08]   Sian Barris and Chris Button. "A Review of Vision-Based Motion Analysis in
            Sport". In: *Sports Medicine* 38.12 (Dec. 1, 2008), pp. 1025–1043. ISSN: 1179-
            2035. DOI: 10.2165/00007256-200838120-00006. URL: https://doi.org/10.
            2165/00007256-200838120-00006 (visited on 01/05/2024).

[Boo98]   R. T. Boone and J. G. Cunningham. "Children's decoding of emotion in expressive
            body movement: the development of cue attunement". In: *Developmental Psy-
            chology* 34.5 (Sept. 1998), pp. 1007–1016. ISSN: 0012-1649. DOI: 10.1037//0012-
            1649.34.5.1007.

[Bos23]   Melissa A. Boswell, Łukasz Kidziński, Jennifer L. Hicks, Scott D. Uhlrich, An-
            toine Falisse, and Scott L. Delp. "Smartphone videos of the sit-to-stand test
            predict osteoarthritis and health outcomes in a nationwide study". In: *npj Digital
            Medicine* 6.1 (Mar. 4, 2023). Number: 1 Publisher: Nature Publishing Group,
            pp. 1–7. ISSN: 2398-6352. DOI: 10.1038/s41746-023-00775-1. URL: https:
            //www.nature.com/articles/s41746-023-00775-1 (visited on 01/05/2024).

[Bra04]   H. Stefan Bracha. "Freeze, Flight, Fight, Fright, Faint: Adaptationist Perspectives
            on the Acute Stress Response Spectrum". In: *CNS Spectrums* 9.9 (Sept. 2004).
            Publisher: Cambridge University Press, pp. 679–685. ISSN: 2165-6509, 1092-8529.
            DOI: 10.1017/S1092852900001954. URL: https://www.cambridge.org/core/
            product/%20identifier/S1092852900001954/type/journal_article (visited
            on 01/05/2024).

[Cam03] Antonio Camurri, Barbara Mazzarino, Matteo Ricchetti, R. Timmers, and Gualtiero Volpe. "Multimodal Analysis of Expressive Gesture in Music and Dance Performances". In: Gesture-Based Communication in Human-Computer Interaction. Lecture Notes in Computer Science, 2915. Apr. 15, 2003, pp. 20–39. ISBN: 978-3-540-21072-6. DOI: 10.1007/978-3-540-24598-8_3.

[Cao19] Zhe Cao, Gines Hidalgo, Tomas Simon, Shih-En Wei, and Yaser Sheikh. *Open-Pose: Realtime Multi-Person 2D Pose Estimation using Part Affinity Fields*. May 30, 2019. DOI: 10.48550/arXiv.1812.08008. arXiv: 1812.08008[cs]. URL: http://arxiv.org/abs/1812.08008 (visited on 11/15/2023).

[Car06] George Caridakis, Amaryllis Raouzaiou, Kostas Karpouzis, and Stefanos Kollias. "Synthesizing gesture expressivity based on real sequences". In: *Workshop Programme* 10 (Jan. 1, 2006), p. 19. URL: https://www.researchgate.net/publication/235761681_Synthesizing_gesture_expressivity_based_on_real_sequences.

[Car16] Roger Carpenter. "A Review of Instruments on Cognitive Appraisal of Stress". In: *Archives of Psychiatric Nursing* 30.2 (Apr. 1, 2016), pp. 271–279. ISSN: 0883-9417. DOI: 10.1016/j.apnu.2015.07.002. URL: https://www.sciencedirect.com/science/article/pii/S0883941715001429 (visited on 01/27/2024).

[Cha22] Changjun Zhou. "Assessment of affective valence and intensity when interpreting nonverbal emotional expressive behaviour". In: (Sept. 12, 2022). DOI: 10.31234/osf.io/596hv. URL: https://typeset.io/papers/assessment-of-affective-valence-and-intensity-when-9iwf4v6h (visited on 01/30/2024).

[Cho08] Daniel B. Chorney and Tracy L. Morris. "The changing face of dating anxiety: Issues in assessment with special populations". In: *Clinical Psychology: Science and Practice* 15.3 (2008). Place: United Kingdom Publisher: Wiley-Blackwell Publishing Ltd., pp. 224–238. ISSN: 1468-2850. DOI: 10.1111/j.1468-2850.2008.00132.x.

[Coh07] Sheldon Cohen, Denise Janicki-Deverts, and Gregory E. Miller. "Psychological Stress and Disease". In: *JAMA* 298.14 (Oct. 10, 2007), pp. 1685–1687. ISSN: 0098-7484. DOI: 10.1001/jama.298.14.1685. URL: https://doi.org/10.1001/jama.298.14.1685 (visited on 11/14/2023).

[Col18]   Steffi L. Colyer, Murray Evans, Darren P. Cosker, and Aki I. T. Salo. "A Review of the Evolution of Vision-Based Motion Analysis and the Integration of Advanced Computer Vision Methods Towards Developing a Markerless System". In: *Sports Medicine - Open* 4.1 (June 5, 2018), p. 24. ISSN: 2198-9761. DOI: 10.1186/s40798-018-0139-y. URL: https://doi.org/10.1186/s40798-018-0139-y (visited on 01/26/2024).

[Col94]   John P. Colby, Arnold S. Linsky, and Murray A. Straus. "Social stress and state-to-state differences in smoking and smoking related mortality in the United States". In: *Social Science & Medicine* 38.2 (Jan. 1, 1994), pp. 373–381. ISSN: 0277-9536. DOI: 10.1016/0277-9536(94)90407-3. URL: https://www.sciencedirect.com/science/article/pii/0277953694904073 (visited on 11/14/2023).

[Con81]   T. L. Conway, R. R. Vickers, H. W. Ward, and R. H. Rahe. "Occupational stress and variation in cigarette, coffee, and alcohol consumption". In: *Journal of Health and Social Behavior* 22.2 (June 1981), pp. 155–165. ISSN: 0022-1465. DOI: https://doi.org/10.2307/2136291.

[Dae12]   Nele Dael, Marcello Mortillaro, and Klaus R Scherer. "Emotion expression in body action and posture". In: *Emotion* 12.5 (Oct. 2012). ZSCC: 0000303, pp. 1085–1101. ISSN: 1528-3542. DOI: 10.1037/a0025737. URL: http://dx.doi.org/10.1037/a0025737.

[Dam23]   Matthew Damian Riina, Cassandra Stambaugh, Nathaniel Stambaugh, and Kathryn E. Huber. "Chapter 28 - Continuous variable analyses: t-test, Mann–Whitney, Wilcoxin rank". In: *Translational Radiation Oncology*. Ed. by Adam E. M. Eltorai, Jeffrey A. Bakal, Daniel W. Kim, and David E. Wazer. Handbook for Designing and Conducting Clinical and Translational Research. Academic Press, Jan. 1, 2023, pp. 153–163. ISBN: 978-0-323-88423-5. DOI: 10.1016/B978-0-323-88423-5.00070-4. URL: https://www.sciencedirect.com/science/article/pii/B9780323884235000704 (visited on 02/22/2024).

[Daw16]   Michael E. Dawson, Anne M. Schell, and Diane L. Filion. "The electrodermal system". In: *Handbook of psychophysiology, 4th ed*. Cambridge handbooks in psychology. New York, NY, US: Cambridge University Press, 2016, pp. 217–243. ISBN: 978-1-107-05852-1 978-1-316-72858-1. URL: https://doi.org/10.1017/9781107415782.010.

[Dou18]   Michail Doumas, Kinga Morsanyi, and William R. Young. "Cognitively and socially induced stress affects postural control". In: *Experimental Brain Research* 236.1 (Jan. 1, 2018), pp. 305–314. ISSN: 1432-1106. DOI: 10.1007/s00221-017-5128-8. URL: https://doi.org/10.1007/s00221-017-5128-8 (visited on 01/05/2024).

[Duc12]   A. Duchesne, E. Tessera, K. Dedovic, V. Engert, and J. C. Pruessner. "Effects of panel sex composition on the physiological stress responses to psychosocial stress in healthy young men and women". In: *Biological Psychology* 89.1 (Jan. 1, 2012), pp. 99–106. ISSN: 0301-0511. DOI: 10.1016/j.biopsycho.2011.09.009. URL: https://www.sciencedirect.com/science/article/pii/S0301051111002432 (visited on 02/21/2024).

[Eil05]   David Eilam. "Die hard: A blend of freezing and fleeing as a dynamic defense—implications for the control of defensive behavior". In: *Neuroscience & Biobehavioral Reviews*. Defensive Behavior 29.8 (Jan. 1, 2005), pp. 1181–1191. ISSN: 0149-7634. DOI: 10.1016/j.neubiorev.2005.03.027. URL: https://www.sciencedirect.com/science/article/pii/S0149763405000643 (visited on 01/05/2024).

[Fan21]   Jinlong Fan, Jing Zhang, Stephen J. Maybank, and Dacheng Tao. *Wide-angle Image Rectification: A Survey*. Dec. 1, 2021. DOI: 10.48550/arXiv.2011.12108. arXiv: 2011.12108[cs,eess]. URL: http://arxiv.org/abs/2011.12108 (visited on 02/27/2024).

[Fan23]   Hao-Shu Fang, Jiefeng Li, Hongyang Tang, Chao Xu, Haoyi Zhu, Yuliang Xiu, Yong-Lu Li, and Cewu Lu. "AlphaPose: Whole-Body Regional Multi-Person Pose Estimation and Tracking in Real-Time". In: *IEEE Transactions on Pattern Analysis and Machine Intelligence* 45.6 (June 2023). Conference Name: IEEE Transactions on Pattern Analysis and Machine Intelligence, pp. 7157–7173. ISSN: 1939-3539. DOI: 10.1109/TPAMI.2022.3222784. URL: https://ieeexplore.ieee.org/document/9954214 (visited on 11/15/2023).

[Fur17]   Daisuke Furuki and Ken Takiyama. "Detecting the relevance to performance of whole-body movements". In: *Scientific Reports* 7.1 (Nov. 15, 2017). Publisher: Nature Publishing Group, p. 15659. ISSN: 2045-2322. DOI: 10.1038/s41598-017-

15888-3. URL: https://www.nature.com/articles/s41598-017-15888-3 (visited on 03/08/2024).

[Gaa09] J. Gaab. "PASA – Primary Appraisal Secondary Appraisal - Ein Fragebogen zur Erfassung von situations-bezogenen kognitiven Bewertungen". In: *Verhaltenstherapie* 19.2 (July 2009). Number: 2 Publisher: Karger, pp. 114–115. ISSN: 1016-6262. DOI: 10.1159/000223610. URL: https://www.zora.uzh.ch/id/eprint/24570/ (visited on 01/27/2024).

[Gel15] B. de Gelder, A.w. de Borst, and R. Watson. "The perception of emotion in body expressions". In: *WIREs Cognitive Science* 6.2 (2015). _eprint: https://onlinelibrary.wiley.com/doi/pdf/10.1002/wcs.1335, pp. 149–158. ISSN: 1939-5086. DOI: 10.1002/wcs.1335. URL: https://onlinelibrary.wiley.com/doi/abs/10.1002/wcs.1335 (visited on 12/14/2023).

[Geß23] Geßler, Tobias. "openTSST – An Open Web Platform for Large-Scale, Video-Based Motion Analysis During Acute Psychosocial Stress". Bachelor Thesis. Friedrich-Alexander-Universität Erlangen-Nürnberg, 2023. URL: https://www.mad.tf.fau.de/files/2023/08/BA_Gessler_Tobias.pdf.

[Gia12] Dimitris Giakoumis, Anastasios Drosou, Pietro Cipresso, Dimitrios Tzovaras, George Hassapis, Andrea Gaggioli, and Giuseppe Riva. "Using Activity-Related Behavioural Features towards More Effective Automatic Stress Detection". In: *PLOS ONE* 7.9 (Sept. 19, 2012). Publisher: Public Library of Science, e43571. ISSN: 1932-6203. DOI: 10.1371/journal.pone.0043571. URL: https://journals.plos.org/plosone/article?id=10.1371/journal.pone.0043571 (visited on 12/19/2023).

[Gia17] G. Giannakakis, M. Pediaditis, D. Manousos, E. Kazantzaki, F. Chiarugi, P.G. Simos, K. Marias, and M. Tsiknakis. "Stress and anxiety detection using facial cues from videos". In: *Biomedical Signal Processing and Control* 31 (Jan. 2017), pp. 89–101. ISSN: 17468094. DOI: 10.1016/j.bspc.2016.06.020. URL: https://linkinghub.elsevier.com/retrieve/pii/S1746809416300805 (visited on 01/01/2023).

[Glo11] Donald Glowinski, Nele Dael, Antonio Camurri, Gualtiero Volpe, Marcello Mortillaro, and Klaus Scherer. "Toward a Minimal Representation of Affective Ges-

tures". In: *IEEE Transactions on Affective Computing* 2.2 (Apr. 2011). Conference Name: IEEE Transactions on Affective Computing, pp. 106–118. ISSN: 1949-3045. DOI: 10.1109/T-AFFC.2011.7. URL: https://ieeexplore.ieee.org/document/5740837 (visited on 12/22/2023).

[Goo17]   William K. Goodman, Johanna Janson, and Jutta M. Wolf. "Meta-analytical assessment of the effects of protocol variations on cortisol responses to the Trier Social Stress Test". In: *Psychoneuroendocrinology* 80 (June 1, 2017), pp. 26–35. ISSN: 0306-4530. DOI: 10.1016/j.psyneuen.2017.02.030. URL: https://www.sciencedirect.com/science/article/pii/S0306453016309702 (visited on 11/15/2023).

[Hag14]   Muriel A. Hagenaars, Karin Roelofs, and John F. Stins. "Human freezing in response to affective films". In: *Anxiety, Stress, & Coping* 27.1 (Jan. 2, 2014). Publisher: Routledge _eprint: https://doi.org/10.1080/10615806.2013.809420, pp. 27–37. ISSN: 1061-5806. DOI: 10.1080/10615806.2013.809420. URL: https://doi.org/10.1080/10615806.2013.809420 (visited on 12/09/2023).

[Hal21]   Uriel Halbreich. "Stress-related physical and mental disorders: a new paradigm". In: *BJPsych Advances* 27.3 (May 2021). Publisher: Cambridge University Press, pp. 145–152. ISSN: 2056-4678, 2056-4686. DOI: 10.1192/bja.2021.1. (Visited on 11/14/2023).

[Ham20]   Ajna Hamidovic, Kristina Karapetyan, Fadila Serdarevic, So Hee Choi, Tory Eisenlohr-Moul, and Graziano Pinna. "Higher Circulating Cortisol in the Follicular vs. Luteal Phase of the Menstrual Cycle: A Meta-Analysis". In: *Frontiers in Endocrinology* 11 (2020). ISSN: 1664-2392. DOI: https://doi.org/10.3389/fendo.2020.00311. URL: https://www.frontiersin.org/journals/endocrinology/articles/10.3389/fendo.2020.00311 (visited on 02/09/2024).

[Hap13]   U. Hapke, U.E. Maske, C. Scheidt-Nave, L. Bode, R. Schlack, and M.A. Busch. "Chronischer Stress bei Erwachsenen in Deutschland". In: *Bundesgesundheitsblatt - Gesundheitsforschung - Gesundheitsschutz* 56.5 (May 1, 2013), pp. 749–754. ISSN: 1437-1588. DOI: 10.1007/s00103-013-1690-9. URL: https://doi.org/10.1007/s00103-013-1690-9 (visited on 11/14/2023).

[Het09]   S. Het, N. Rohleder, D. Schoofs, C. Kirschbaum, and O.T. Wolf. "Neuroendocrine and psychometric evaluation of a placebo version of the 'Trier Social Stress Test'". In: *Psychoneuroendocrinology* 34.7 (Aug. 2009), pp. 1075–1086. ISSN: 03064530. DOI: 10.1016/j.psyneuen.2009.02.008. URL: https://linkinghub.elsevier.com/retrieve/pii/S0306453009000614 (visited on 01/18/2022).

[Jar18]   Delaram Jarchi, James Pope, Tracey K. M. Lee, Larisa Tamjidi, Amirhosein Mirzaei, and Saeid Sanei. "A Review on Accelerometry-Based Gait Analysis and Emerging Clinical Applications". In: *IEEE Reviews in Biomedical Engineering* 11 (2018). Conference Name: IEEE Reviews in Biomedical Engineering, pp. 177–194. ISSN: 1941-1189. DOI: 10.1109/RBME.2018.2807182. URL: https://ieeexplore.ieee.org/document/8293814 (visited on 01/05/2024).

[Kir93]   Clemens Kirschbaum, Karl-Martin Pirke, and Dirk H. Hellhammer. "The 'Trier Social Stress Test' – A Tool for Investigating Psychobiological Stress Responses in a Laboratory Setting". In: *Neuropsychobiology*. Vol. 28. Issue: 1-2 ISSN: 0302282X. 1993, pp. 76–81. ISBN: 978-0-87421-656-1. DOI: 10.1159/000119004.

[Kle13]   Andrea Kleinsmith and Nadia Bianchi-Berthouze. "Affective Body Expression Perception and Recognition: A Survey". In: *Affective Computing, IEEE Transactions on* 4 (Jan. 1, 2013), pp. 15–33. DOI: 10.1109/T-AFFC.2012.16.

[Krü13]   Samuel Krüger, Alexander N. Sokolov, Paul Enck, Ingeborg Krägeloh-Mann, and Marina A. Pavlova. "Emotion through Locomotion: Gender Impact". In: *PLoS ONE* 8.11 (Nov. 22, 2013), e81716. ISSN: 1932-6203. DOI: 10.1371/journal.pone.0081716. URL: https://www.ncbi.nlm.nih.gov/pmc/articles/PMC3838416/ (visited on 01/30/2024).

[Lab19]   Izelle Labuschagne, Caitlin Grace, Peter Rendell, Gill Terrett, and Markus Heinrichs. "An introductory guide to conducting the Trier Social Stress Test". In: *Neuroscience & Biobehavioral Reviews* 107 (Dec. 2019), pp. 686–695. ISSN: 01497634. DOI: 10.1016/j.neubiorev.2019.09.032. URL: https://linkinghub.elsevier.com/retrieve/pii/S0149763419308255 (visited on 07/24/2021).

[Las20]   J. Lasselin, T. Sundelin, P. M. Wayne, M. J. Olsson, S. Paues Göranson, J. Axelsson, and M. Lekander. "Biological motion during inflammation in humans". In:

Brain, Behavior, and Immunity 84 (Feb. 2020), pp. 147–153. ISSN: 1090-2139. DOI: 10.1016/j.bbi.2019.11.019.

[Lef16] Iulia Lefter, Gertjan J. Burghouts, and Léon J.M. Rothkrantz. "Recognizing Stress Using Semantics and Modulation of Speech and Gestures". In: *IEEE Transactions on Affective Computing* 7.2 (Apr. 2016). Conference Name: IEEE Transactions on Affective Computing, pp. 162–175. ISSN: 1949-3045. DOI: 10.1109/TAFFC.2015.2451622. URL: https://ieeexplore.ieee.org/document/7145400 (visited on 12/19/2023).

[Löw15] Andreas Löw, Mathias Weymar, and Alfons O. Hamm. "When Threat Is Near, Get Out of Here: Dynamics of Defensive Behavior During Freezing and Active Avoidance". In: *Psychological Science* 26.11 (Nov. 1, 2015). Publisher: SAGE Publications Inc, pp. 1706–1716. ISSN: 0956-7976. DOI: 10.1177/0956797615597332. URL: https://doi.org/10.1177/0956797615597332 (visited on 01/05/2024).

[May19] Leah M. Mayo and Markus Heilig. "In the face of stress: Interpreting individual differences in stress-induced facial expressions". In: *Neurobiology of Stress* 10 (Feb. 2019), p. 100166. ISSN: 23522895. DOI: 10.1016/j.ynstr.2019.100166. URL: https://linkinghub.elsevier.com/retrieve/pii/S2352289518300985 (visited on 11/15/2022).

[McC91] J. A. McCubbin, J. F. Wilson, S. Bruehl, M. Brady, K. Clark, and E. Kort. "Gender effects on blood pressures obtained during an on-campus screening." In: *Psychosomatic Medicine* 53.1 (Feb. 1991), p. 90. ISSN: 0033-3174. DOI: https://doi.org/10.1097/00006842-199101000-00008. URL: https://journals.lww.com/psychosomaticmedicine/Abstract/1991/01000/Gender_effects_on_blood_pressures_obtained_during.8.aspx (visited on 02/21/2024).

[McE93] Bruce S. McEwen and Eliot Stellar. "Stress and the Individual: Mechanisms Leading to Disease". In: *Archives of Internal Medicine* 153.18 (Sept. 27, 1993), pp. 2093–2101. ISSN: 0003-9926. DOI: 10.1001/archinte.1993.00410180039004. URL: https://doi.org/10.1001/archinte.1993.00410180039004 (visited on 11/14/2023).

[Mik20] Daisuke Miki, Shinya Abe, Shi Chen, and Kazuyuki Demachi. "Robust human pose estimation from distorted wide-angle images through iterative search of

transformation parameters". In: *Signal, Image and Video Processing* 14.4 (June 1, 2020), pp. 693–700. ɪssɴ: 1863-1711. ᴅᴏɪ: 10.1007/s11760-019-01602-5. ᴜʀʟ: https://doi.org/10.1007/s11760-019-01602-5 (visited on 02/27/2024).

[Mil02]   Diane B. Miller and James P. O'Callaghan. "Neuroendocrine aspects of the response to stress". In: *Metabolism: Clinical and Experimental* 51.6 (June 2002), pp. 5–10. ɪssɴ: 0026-0495. ᴅᴏɪ: 10.1053/meta.2002.33184.

[Miu20]   Teppei Miura and Shinji Sako. "3D human pose estimation model using location-maps for distorted and disconnected images by a wearable omnidirectional camera". In: *IPSJ Transactions on Computer Vision and Applications* 12.1 (Aug. 31, 2020), p. 4. ɪssɴ: 1882-6695. ᴅᴏɪ: 10.1186/s41074-020-00066-8. ᴜʀʟ: https://doi.org/10.1186/s41074-020-00066-8 (visited on 02/27/2024).

[Nat09]   U. M. Nater and N. Rohleder. "Salivary alpha-amylase as a non-invasive biomarker for the sympathetic nervous system: Current state of research". In: *Psychoneuroendocrinology* 34.4 (May 1, 2009), pp. 486–496. ɪssɴ: 0306-4530. ᴅᴏɪ: 10.1016/j.psyneuen.2009.01.014. ᴜʀʟ: https://www.sciencedirect.com/science/article/pii/S0306453009000328 (visited on 11/15/2023).

[Nim12]   Ashish D. Nimbarte, Mohammed J. Al Hassan, Steve E. Guffey, and Warren R. Myers. "Influence of psychosocial stress and personality type on the biomechanical loading of neck and shoulder muscles". In: *International Journal of Industrial Ergonomics* 42.5 (Sept. 1, 2012), pp. 397–405. ɪssɴ: 0169-8141. ᴅᴏɪ: 10.1016/j.ergon.2012.05.001. ᴜʀʟ: https://www.sciencedirect.com/science/article/pii/S0169814112000467 (visited on 02/23/2024).

[Nol23]   Noldus Information Technology. *FaceReader: A robust automated system for facial expressions analysis*. 2023. ᴜʀʟ: https://www.noldus.com/facereader.

[Noo20]   Marret K. Noordewier, Daan T. Scheepers, and Leon P. Hilbert. "Freezing in response to social threat: a replication". In: *Psychological Research* 84.7 (Oct. 1, 2020), pp. 1890–1896. ɪssɴ: 1430-2772. ᴅᴏɪ: 10.1007/s00426-019-01203-4. ᴜʀʟ: https://doi.org/10.1007/s00426-019-01203-4 (visited on 12/10/2023).

[OCo21]   Daryl B. O'Connor, Julian F. Thayer, and Kavita Vedhara. "Stress and Health: A Review of Psychobiological Processes". In: *Annual Review of Psychology* 72.1 (2021). _eprint: https://doi.org/10.1146/annurev-psych-062520-122331, pp. 663–

688. DOI: 10.1146/annurev-psych-062520-122331. URL: https://doi.org/10.1146/annurev-psych-062520-122331 (visited on 11/14/2023).

[Par22]   Antonis Pardos, Melina Tziomaka, Andreas Menychtas, and Ilias Maglogiannis. "Automated Posture Analysis for the Assessment of Sports Exercises". In: *Proceedings of the 12th Hellenic Conference on Artificial Intelligence*. SETN '22. New York, NY, USA: Association for Computing Machinery, Sept. 9, 2022, pp. 1–9. ISBN: 978-1-4503-9597-7. DOI: 10.1145/3549737.3549784. URL: https://dl.acm.org/doi/10.1145/3549737.3549784 (visited on 01/05/2024).

[Pea08]   Jennifer Peat and Belinda Barton. *Medical Statistics: A Guide to Data Analysis and Critical Appraisal*. Google-Books-ID: NHiDnKiDajEC. John Wiley & Sons, Apr. 15, 2008. 339 pp. ISBN: 978-0-470-75520-4.

[Pru03]   Jens C. Pruessner, Clemens Kirschbaum, Gunther Meinlschmid, and Dirk H Hellhammer. "Two formulas for computation of the area under the curve represent measures of total hormone concentration versus time-dependent change". In: *Psychoneuroendocrinology* 28.7 (Oct. 1, 2003), pp. 916–931. ISSN: 0306-4530. DOI: 10.1016/S0306-4530(02)00108-7. URL: https://www.sciencedirect.com/science/article/pii/S0306453002001087 (visited on 02/20/2024).

[Ran20]   Keerthana Rangasamy, Muhammad Amir As'ari, Nur Azmina Rahmad, Nurul Fathiah Ghazali, and Saharudin Ismail. "Deep learning in sport video analysis: a review". In: *TELKOMNIKA (Telecommunication Computing Electronics and Control)* 18.4 (Aug. 1, 2020). Number: 4, pp. 1926–1933. ISSN: 2302-9293. DOI: 10.12928/telkomnika.v18i4.14730. URL: http://telkomnika.uad.ac.id/index.php/TELKOMNIKA/article/view/14730 (visited on 01/05/2024).

[Ric21]   Robert Richer, Arne Küderle, Martin Ullrich, Nicolas Rohleder, and Bjoern M. Eskofier. "BioPsyKit: A Python package for the analysis of biopsychological data". In: *Journal of Open Source Software* 6.66 (Oct. 12, 2021), p. 3702. ISSN: 2475-9066. DOI: 10.21105/joss.03702. URL: https://joss.theoj.org/papers/10.21105/joss.03702 (visited on 11/30/2023).

[Ric24]   Robert Richer, Veronika Koch, Luca Abel, Felicitas Hauck, Miriam Kurz, Veronika Ringgold, Arne Kürderle, Lena Schindler-Gmelch, Nicolas Rohleder, and Bjoern M. Eskofier. "Machine Learning-based Detection of Acute Psychosocial Stress

from Body Posture and Movements". In: *Scientific Reports (Submitted to review)* (2024).

[Roe09]   Daniel Roetenberg, Henk Luinge, and Per Slycke. "Xsens MVN: Full 6DOF human motion tracking using miniature inertial sensors". In: *Xsens Motion Technol. BV Tech. Rep.* 3 (Jan. 1, 2009). URL: https://www.researchgate.net/publication/239920367_Xsens_MVN_Full_6DOF_human_motion_tracking_using_miniature_inertial_sensors.

[Roe10]   Karin Roelofs, Muriel A. Hagenaars, and John Stins. "Facing Freeze: Social Threat Induces Bodily Freeze in Humans". In: *Psychological Science* 21.11 (Nov. 1, 2010). Publisher: SAGE Publications Inc, pp. 1575–1581. ISSN: 0956-7976. DOI: 10.1177/0956797610384746. URL: https://doi.org/10.1177/0956797610384746 (visited on 11/10/2023).

[Roe17]   Karin Roelofs. "Freeze for action: neurobiological mechanisms in animal and human freezing". In: *Philosophical Transactions of the Royal Society B: Biological Sciences* 372.1718 (Feb. 27, 2017). Publisher: Royal Society, p. 20160206. DOI: 10.1098/rstb.2016.0206. URL: https://royalsocietypublishing.org/doi/10.1098/rstb.2016.0206 (visited on 12/10/2023).

[Roh19]   Nicolas Rohleder. "Stress and inflammation – The need to address the gap in the transition between acute and chronic stress effects". In: *Psychoneuroendocrinology*. Festschrift for Dirk Hellhammer 105 (July 1, 2019), pp. 164–171. ISSN: 0306-4530. DOI: 10.1016/j.psyneuen.2019.02.021. URL: https://www.sciencedirect.com/science/article/pii/S0306453018306954 (visited on 11/15/2023).

[Sch05]   Neil Schneiderman, Gail Ironson, and Scott D. Siegel. "STRESS AND HEALTH: Psychological, Behavioral, and Biological Determinants". In: *Annual review of clinical psychology* 1 (2005), pp. 607–628. ISSN: 1548-5943. DOI: 10.1146/annurev.clinpsy.1.102803.144141. URL: https://www.ncbi.nlm.nih.gov/pmc/articles/PMC2568977/ (visited on 11/14/2023).

[Sha13]   Bahar Shahidi, Ashley Haight, and Katrina Maluf. "Differential effects of mental concentration and acute psychosocial stress on cervical muscle activity and posture". In: *Journal of Electromyography and Kinesiology* 23.5 (Oct. 1, 2013), pp. 1082–1089. ISSN: 1050-6411. DOI: 10.1016/j.jelekin.2013.05.009. URL:

https://www.sciencedirect.com/science/article/pii/S1050641113001235 (visited on 11/07/2023).

[Sin18]   Jasvinder Pal Singh, Sanjeev Jain, Sakshi Arora, and Uday Pratap Singh. "Vision-Based Gait Recognition: A Survey". In: *IEEE Access* 6 (2018). Conference Name: IEEE Access, pp. 70497–70527. ISSN: 2169-3536. DOI: 10.1109/ACCESS.2018.2879896. URL: https://ieeexplore.ieee.org/document/8528404 (visited on 01/05/2024).

[Sla15]   Danica C. Slavish, Jennifer E. Graham-Engeland, Joshua M. Smyth, and Christopher G. Engeland. "Salivary markers of inflammation in response to acute stress". In: *Brain, Behavior, and Immunity* 44 (Feb. 1, 2015), pp. 253–269. ISSN: 0889-1591. DOI: 10.1016/j.bbi.2014.08.008. URL: https://www.sciencedirect.com/science/article/pii/S0889159114004255 (visited on 11/15/2023).

[Sok11]   Arseny Sokolov, Samuel Krüger, Paul Enck, Ingeborg Krägeloh-Mann, and Marina Pavlova. "Gender Affects Body Language Reading". In: *Frontiers in Psychology* 2 (2011). ISSN: 1664-1078. URL: https://www.frontiersin.org/articles/10.3389/fpsyg.2011.00016 (visited on 01/30/2024).

[Ste21]   Jan Stenum, Cristina Rossi, and Ryan T. Roemmich. "Two-dimensional video-based analysis of human gait using pose estimation". In: *PLOS Computational Biology* 17.4 (Apr. 23, 2021). Publisher: Public Library of Science, e1008935. ISSN: 1553-7358. DOI: 10.1371/journal.pcbi.1008935. URL: https://journals.plos.org/ploscompbiol/article?id=10.1371/journal.pcbi.1008935 (visited on 01/05/2024).

[Sum23]   Himanshu Kumar Suman and Tanmay Tulsidas Verlekar. "Video-Based Gait Analysis for Spinal Deformity". In: *Computer Vision – ECCV 2022 Workshops*. Ed. by Leonid Karlinsky, Tomer Michaeli, and Ko Nishino. Lecture Notes in Computer Science. Cham: Springer Nature Switzerland, 2023, pp. 278–288. ISBN: 978-3-031-25072-9. DOI: 10.1007/978-3-031-25072-9_18.

[Ter10]   Vasileios Terzis, Christos N. Moridis, and Anastasios A. Economides. "Measuring instant emotions during a self-assessment test: the use of FaceReader". In: *Proceedings of the 7th International Conference on Methods and Techniques in Behavioral Research*. MB '10. New York, NY, USA: Association for Computing

Machinery, Aug. 24, 2010, pp. 1–4. ISBN: 978-1-60558-926-8. DOI: 10.1145/1931344.1931362. URL: https://doi.org/10.1145/1931344.1931362 (visited on 01/05/2024).

[Val18] Raphael Vallat. "Pingouin: statistics in Python". In: *Journal of Open Source Software* 3.31 (Nov. 19, 2018), p. 1026. ISSN: 2475-9066. DOI: 10.21105/joss.01026. URL: https://joss.theoj.org/papers/10.21105/joss.01026 (visited on 02/13/2024).

[Vri97] Aldert Vrij, Lucy Akehurst, and Paul Morris. "Individual Differences in Hand Movements During Deception". In: *Journal of Nonverbal Behavior* 21.2 (June 1, 1997), pp. 87–102. ISSN: 1573-3653. DOI: 10.1023/A:1024951902752. URL: https://doi.org/10.1023/A:1024951902752 (visited on 01/04/2024).

[Wal98] Harald G. Wallbott. "Bodily expression of emotion". In: *European Journal of Social Psychology* 28.6 (1998), pp. 879–896. ISSN: 1099-0992. DOI: https://doi.org/10.1002/(SICI)1099-0992(1998110)28:6%3C879::AID-EJSP901%3E3.0.CO;2-W. (Visited on 01/03/2024).

[Wan19] Jianbo Wang, Kai Qiu, Houwen Peng, Jianlong Fu, and Jianke Zhu. "AI Coach: Deep Human Pose Estimation and Analysis for Personalized Athletic Training Assistance". In: *Proceedings of the 27th ACM International Conference on Multimedia*. MM '19. New York, NY, USA: Association for Computing Machinery, Oct. 15, 2019, pp. 374–382. ISBN: 978-1-4503-6889-6. DOI: 10.1145/3343031.3350910. URL: https://doi.org/10.1145/3343031.3350910 (visited on 01/05/2024).

[Was05] Jeanette Wasserstein. "Diagnostic issues for adolescents and adults with ADHD". In: *Journal of Clinical Psychology* 61.5 (2005). _eprint: https://onlinelibrary.wiley.com/doi/pdf/10.1002/jclp.20118, pp. 535–547. ISSN: 1097-4679. DOI: 10.1002/jclp.20118. URL: https://onlinelibrary.wiley.com/doi/abs/10.1002/jclp.20118 (visited on 02/24/2024).

[Wer18] Philipp Werner, Ayoub Al-Hamadi, Kerstin Limbrecht-Ecklundt, Steffen Walter, and Harald C Traue. "Head movements and postures as pain behavior". In: *PLoS One* 13.2 (Feb. 14, 2018), e0192767. ISSN: 1932-6203. DOI: 10.1371/journal.pone.0192767. URL: http://dx.doi.org/10.1371/journal.pone.0192767.

[Wie13]   Uta S. Wiemers, Daniela Schoofs, and Oliver T. Wolf. "A friendly version of
            the Trier Social Stress Test does not activate the HPA axis in healthy men and
            women". In: *Stress* 16.2 (Mar. 2013), pp. 254–260. ISSN: 1025-3890, 1607-8888.
            DOI: 10.3109/10253890.2012.714427. URL: 10.3109/10253890.2012.714427
            (visited on 10/17/2020).

[Wij10]   Jacqueline Wijsman, Bernard Grundlehner, Julien Penders, and Hermie Hermens.
            "Trapezius Muscle EMG as Predictor of Mental Stress". In: ACM Transactions
            on Embedded Computing Systems (TECS). Vol. 12. Oct. 5, 2010, pp. 155–163.
            DOI: 10.1145/2485984.2485987.

[Wil08]   Barry D. Wilson. "Development in video technology for coaching". In: *Sports
            Technology* 1.1 (Jan. 1, 2008), pp. 34–40. ISSN: 1934-6182. DOI: 10.1080/
            19346182.2008.9648449. (Visited on 01/05/2024).

[Wil45]   Frank Wilcoxon. "Individual Comparisons by Ranking Methods". In: *Biometrics
            Bulletin* 1.6 (1945). Publisher: [International Biometric Society, Wiley], pp. 80–
            83. ISSN: 0099-4987. DOI: 10.2307/3001968. URL: https://www.jstor.org/
            stable/3001968 (visited on 02/22/2024).

[Ye22]   Run Zhou Ye, Arun Subramanian, Daniel Diedrich, Heidi Lindroth, Brian Picker-
            ing, and Vitaly Herasevich. "Effects of Image Quality on the Accuracy Human
            Pose Estimation and Detection of Eye Lid Opening/Closing Using Openpose and
            DLib". In: *Journal of Imaging* 8.12 (Dec. 19, 2022), p. 330. ISSN: 2313-433X.
            DOI: 10.3390/jimaging8120330. URL: https://www.ncbi.nlm.nih.gov/pmc/
            articles/PMC9783075/ (visited on 02/27/2024).

[Yu17]   Chia-Yin Yu and Chih-Hsiang Ko. "Applying FaceReader to Recognize Consumer
            Emotions in Graphic Styles". In: *Procedia CIRP*. Complex Systems Engineering
            and Development Proceedings of the 27th CIRP Design Conference Cranfield
            University, UK 10th – 12th May 2017 60 (Jan. 1, 2017), pp. 104–109. ISSN: 2212-
            8271. DOI: 10.1016/j.procir.2017.01.014. URL: https://www.sciencedirect.
            com/science/article/pii/S221282711730015X (visited on 01/05/2024).

[Zän20]   Sandra Zänkert, Brigitte M. Kudielka, and Stefan Wüst. "Effect of sugar admin-
            istration on cortisol responses to acute psychosocial stress". In: *Psychoneuroen-
            docrinology* 115 (May 1, 2020), p. 104607. ISSN: 0306-4530. DOI: 10.1016/

j.psyneuen.2020.104607. URL: https://www.sciencedirect.com/science/article/pii/S0306453020300263 (visited on 02/09/2024).

[Zee19]   Sophie van der Zee, Ronald Poppe, Paul J. Taylor, and Ross Anderson. "To freeze or not to freeze: A culture-sensitive motion capture approach to detecting deceit". In: *PLOS ONE* 14.4 (Apr. 12, 2019). Publisher: Public Library of Science, e0215000. ISSN: 1932-6203. DOI: 10.1371/journal.pone.0215000. URL: https://journals.plos.org/plosone/article?id=10.1371/journal.pone.0215000 (visited on 11/10/2023).

[Zha19]   Jin Zhang, Xue Mei, Huan Liu, Shenqiang Yuan, and Tiancheng Qian. "Detecting Negative Emotional Stress Based on Facial Expression in Real Time". In: *2019 IEEE 4th International Conference on Signal and Image Processing (ICSIP)*. 2019 IEEE 4th International Conference on Signal and Image Processing (ICSIP). July 2019, pp. 430–434. DOI: 10.1109/SIPROCESS.2019.8868735. URL: https://ieeexplore.ieee.org/document/8868735 (visited on 12/19/2023).

[Zit19]   Giuseppe Angelo Zito, Kallia Apazoglou, Anisoara Paraschiv-Ionescu, Kamiar Aminian, and Selma Aybek. "Abnormal postural behavior in patients with functional movement disorders during exposure to stress". In: *Psychoneuroendocrinology* 101 (Mar. 1, 2019), pp. 232–239. ISSN: 0306-4530. DOI: 10.1016/j.psyneuen.2018.11.020. URL: https://www.sciencedirect.com/science/article/pii/S0306453018311314 (visited on 12/09/2023).

Appendix C

Acronyms

TSST Trier Social Stress Test

f-TSST friendly-Trier Social Stress Test

(f-)TSST (friendly-)Trier Social Stress Test

HPA hypothalamic-pituitary-adrenal

SNS sympathetic nervous system

α-amylase alpha-amylase

OMC optical motion capturing

IMU inertial measurement unit

ML machine learning

FMD functional movement disorders

DL deep learning

NN neural networks

AI artificial intelligence

BMI Body Mass Index

QoM Quantity of Movement

MaD Lab Machine Learning and Data Analytics Lab

PASA Primary Appraisal Secondary Appraisal

CSV Comma-separated values

PLDs point-light displays

FFT Fast Fourier transform

SD Standard deviation

kNN k-nearest neighbors

SVM Support vector machine

AdaBoost Adaptive Boosting

CV cross-validation

RFE recursive feature elimination

ANOVA analysis of variance

SE Standard error

SP static periods

FOV field of view